Conversion of graded phosphorylation into switch-like nuclear translocation via autoregulatory mechanisms in ERK signaling

（増殖因子刺激に対する ERK の核移行応答は自己制御を伴いスイッチ様に誘導される）

Yuki Shindo

Graduate School of Frontier Bioscience, Osaka University

March 2016

Abstract

The phosphorylation cascade in the extracellular signal-regulated kinase (ERK) pathway is a versatile reaction network motif that can potentially act as a switch, oscillator or memory. Nevertheless, there is accumulating evidence that the phosphorylation response is mostly linear to extracellular signals in mammalian cells. Here, I find that subsequent nuclear translocation gives rise to a switch-like increase in nuclear ERK concentration in response to signal input. The switch-like response disappears in the presence of ERK inhibitor, suggesting the existence of autoregulatory mechanisms for ERK nuclear translocation involved in conversion from a graded to a switch-like response. *In vitro* reconstruction of ERK nuclear translocation indicates that ERK-mediated phosphorylation of nucleoporins regulates ERK translocation. A mathematical model and knockdown experiments suggest a contribution of nucleoporins to regulation of the ERK nuclear translocation response. Taken together, this study provides evidence that nuclear translocation with autoregulatory mechanisms acts as a switch in ERK signaling.

Acknowledgements

I would like to express my deep appreciation to my advisors Dr. Koichi Takahashi at RIKEN QBiC and Dr. Yasushi Sako at RIKEN. Dr. Takahashi accepted me as a student trainee and gave me a great environment, where I was able to devote to research. Dr. Sako always gave me important advices and led the direction of the study. I am also grateful for the help from my collaborators; Prof. Hidetaka Kosako at Tokushima University not only helped me perform *in vitro* import assay, which extensively improved the study, but also encouraged me to overcome the revision processes of the paper (Shindo et al., 2016); Dr. Kazunari Iwamoto at RIKEN IMS helped me perform kinetic modeling; Dr. Kazunari Mouri at RIKEN QBiC and Dr. Kayo Hibino at National Institute for Genetics taught me the basics of biological experiments.

I am grateful to my committee members Prof. Toshio Yanagida, Prof. Takeshi Yagi, Prof. Hiroshi Sasaki and Prof. Akihiko Ishijima, for their helpful comments and thoughtful criticisms given to this dissertation. I would also like to thank administrative assistants Miki Yamamoto, Ryoko Tanaka, Kaoru Ikegami, Toshiko Sawai, Yu Yamamoto, Sonoko Kitamura, Satoko Kitamura and Eri Taniguchi, for their kind help and support, technical assistants Hiromi Sato and Akiko Kanayama, for technical support for the experiments, without which this dissertation would not have been possible. I would also like to thank my colleagues and friends for every support they have provided.

Last but not the least, I thank my parents Katsuya Shindo, Mariko Shindo, my brother Daichi Shindo, and my wife Eri Hayashi-Shindo, for their warm support and encouragement.

Table of contents

List of figures

List of tables

Chapter 1: General introduction

Motivation

Cells receive information from environment, process them, and produce appropriate responses. How do cells carry out the information processing, or how do cells "think"? In analogy with the neuronal system, non-linear property of subsystems seems to be important to generate higher order and complex behaviors. If it also applies to cellular systems, what kind of molecular modules, such as a sensor, switch, memory and oscillator, are required to drive higher order physiological events, such as cell fate decision? For example, there seems to be a molecular switch where cellular transitions emerge. Characterizing the principles that cells use to process cellular information would be a big challenge in systems biology.

With these goals in mind, this dissertation focused on mammalian ERK (extracellular signal-regulated kinase) MAPK (mitogen-activated protein kinases) signaling, which has been reported to show less intuitive behaviors. The output of the system defined by the level of phosphorylation of ERK displays a graded response, while ERK signaling is a master regulator of cell fate decision. Therefore, I investigated if there is a switch in ERK signaling other than the phosphorylation, and found that the subsequent nuclear translocation behaves like a switch due to ERK-dependent autoregulatory mechanisms. Details of the results are shown in Chapter 2 and 3.

In the rest of this chapter, I will provide a general introduction of ultrasensitive switches in cellular systems and their biological significance, followed by more specific introduction regarding my dissertation, including molecular basis of ERK signaling and problem settings.

Ultrasensitive switches in cellular networks

Diverse types of signal–response elements, such as “buzzers” (ultrasensitive switches), “sniffers” (transient responses), “toggles” (hysteretic switches) and “blinkers” (oscillators) (Tyson et al., 2003) are building blocks of various types of complex systems. These functional components further interact with each other and generate larger networks of great complexity, which produces coordinated and sophisticated system behaviors. Although I believe the elements are equally important and indeed tightly connected to each other, here I will only concentrate on the ultrasensitive switches that most relate to this dissertation.

Ultrasensitive response i.e., switch-like, sigmoidal input–output relation, often appear in diverse cellular systems. The prefix “ultra” means that the response is more sensitive than hyperbolic Michaelian response (Ferrell and Ha, 2014a), which is derived as follows. Let S, X and X^* be concentrations of signal input, inactive and active form of response element, respectively. The rate equation for X^* using low of mass action can be written as follows:

$$\frac{dX^*}{dt} = k_1 S\, X - k_2 X^*$$

$$= k_1 S\, (X_T - X^*) - k_2 X^*$$

where $X_T = X + X^*$ is total amount of response element, k_1 is a rate constant for activation and k_2 is a rate constant for deactivation. At steady state ($dX^*/dt = 0$), a fraction of response element (X_{ss}^*/X_T) is given as:

$$\frac{X_{ss}^*}{X_T} = \frac{S}{(k_2/k_1) + S}$$

$$= \frac{S}{K + S}$$

where X_{ss}^{*} is a concentration of X^{*} at steady state and K is EC_{50} (half maximal effective concentration) of the signal input by which half of the X is activated. This hyperbolic response is called Michaelian response because the form of the equation is the same as Michaelis-Menten (MM) equation. More generally, Michaelian response can be written as follows.

$$Output = \frac{Input}{EC_{50} + Input}$$

Note that the Michaelian response is generated by systems in which rate equations are described using low of mass action, not MM equations. If the system consists of rate equations described by MM equations, input–output relation of the system would not always be hyperbolic due to the effect of saturation.

In contrast to the hyperbolic property of Michaelian response, ultrasensitive response is sigmoidal and switch-like. The input–output relation is characterized by the Hill function

$$Output = \frac{Input^{n_H}}{EC_{50}^{n_H} + Input^{n_H}}$$

where n_H is the Hill coefficient that determine the steepness of responses. When $n_H > 1$, the response is ultrasensitive, which means that small changes in the input can lead large changes in the output. The greater the n_H becomes, the more switch-like the system behaves. Although there might not be an exact definition, responses that have approximately two or higher value of n_H is often referred to as "switch-like". In contrast, responses with smaller value of n_H is sometimes called "graded" responses.

There are several mechanisms that can generate switch-like responses, including multi-step reactions, saturation (zero-order ultrasensitivity), stoichiometric inhibitors, feedback and feedforward (Ferrell and Ha, 2014a, 2014b; Qian, 2012; Tyson et al., 2003; Zhang et al., 2013).

Although I will not provide the detailed review for these mechanisms, I note that the feedback and feedforward, or more generally, autoregulatory mechanism, is one of the most frequently observed motifs in various cellular networks.

Cell fate decision and switches

Precise regulation of cell fates is crucial for life. In response to extracellular and intracellular signals, cells would select their fates; e.g., proliferation to proceed development or to heal a wound; differentiation to construct the neuronal system or to make immune cells; death to form proper tissue morphology or to ensure cell turnover (Götz and Huttner, 2005; Luckheeram et al., 2012; Pellettieri and Alvarado, 2007; Velnar et al., 2009; Wood et al., 2000). Cell fate decision is ultimately the matter of "to be or not to be", where sharp state transition should emerge. Nevertheless, environmental conditions are usually continuous and have broad ranges of signals, and it is therefore expected that there are some systems that convert a graded input into a switch-like output. Otherwise, cells would waver. The ultrasensitive switch-like property of biochemical networks is a basis for the conversion and plays an important role in many cellular processes, including cell fate decision. Progesterone-induced phosphorylation of p42-MAPK in *Xenopus laevis* oocytes that triggers maturation, G1 cyclins expression in yeast that governs cell cycle entry, and NF-κB activation in B cell receptor signaling that determine B cell functions, are the examples of molecular switches (Ferrell and Machleder, 1998; Shinohara et al., 2014; Skotheim et al., 2008).

Background

As stated above, ultrasensitive switches are important signal–response elements by which a graded signal is converted into switch-like information, and are observed in actual cellular systems. Here in this dissertation, I have investigated mammalian ERK signaling with regard to the (ultra-)sensitivity to the signal input. Intriguingly, the system output defined by the level of phosphorylation of ERK is known to show a graded response while ERK signaling regulates cell fate decision; details are described below.

MAPKs are evolutionally conserved protein kinases that regulate diverse cellular processes, such as cell proliferation, differentiation, apoptosis, survival and tumorigenesis (Chang and Karin, 2001; Qi and Elion, 2005; Roux and Blenis, 2004; Widmann et al., 1999). Although five MAPK families (ERK1/2, JNK (Jun N-terminal kinase), p38, ERK3/4 and ERK5) have been identified in mammalian cells, ERK1/2 (hereafter referred to as ERK for simplicity) pathway, also known as classical MAPK pathway, is the most famous and characterized to date. Upon receipt of a mitogenic signal, ERK is activated by dual-phosphorylation and catalyzes the phosphorylation of numerous proteins, resulting in changes in cell physiology.

The ERK pathway consists of a three-tier phosphorylation cascade with multistep reactions and feedback loops, that inherently generate various behaviors including ultrasensitivity, oscillation and memory (Huang and Ferrell, 1996; Kholodenko, 2000; Markevich et al., 2004; Qiao et al., 2007). An ultrasensitive switch-like response of ERK phosphorylation was actually reported in *Xenopus* oocytes (Ferrell and Machleder, 1998; Xiong and Ferrell, 2003). Such non-linear properties seem to be appropriate for mediating cellular processes where the state transition

emerges. In contrast, a graded response of ERK phosphorylation was observed in mammalian cells (MacKeigan et al., 2005; Perrett et al., 2013; Santos et al., 2007; Whitehurst et al., 2004), which suggests that there may be additional mechanisms other than phosphorylation that digitize the graded ERK signal (Caunt and McArdle, 2012).

Although the kinase activity of ERK itself is regulated by dual-phosphorylation on a TEY activation loop, ERK-driven physiological events require more than phosphorylation. Indeed, ERK accumulates in the nucleus after stimulus-induced phosphorylation, and this nuclear translocation is essential for ERK-mediated processes, such as entry into S-phase (Brunet et al., 1999). Moreover, inhibition of ERK nuclear translocation was recently proposed as a target for anti-cancer therapy (Plotnikov et al., 2015). That is, the output of ERK signaling could be understood in terms of the level of nuclear translocation. Recent studies have demonstrated that there is not a simple correlation between the kinetics of phosphorylation and nuclear translocation (Ahmed et al., 2014; Caunt and McArdle, 2010), suggesting that regulation of ERK translocation is complex and somewhat distinct from phosphorylation.

Translocation of molecules across the nuclear envelope is mediated by the nuclear pore complex (NPC), which is a large protein complex consisting of approximately 30 types of nucleoporins (Nups) (Wente and Rout, 2010). Approximately one third of all Nups contain phenylalanine-glycine repeat regions (FG Nups), which are natively unfolded and form a meshwork or brushwork in the central tube of the NPC that acts as a permeability barrier for non-specific translocation of molecules across the nuclear envelope (Frey and Görlich, 2007; Patel et al., 2007). Karyopherins, such as importins and exportins, bind FG Nups and therefore pass through the barrier of the NPC.

Indeed, ERK can bind directly to the FG repeat region (Lee et al., 2004) and pass through the NPC without carriers (Matsubayashi et al., 2001; Whitehurst et al., 2002), although a carrier-dependent pathway has also been reported (Lorenzen et al., 2001; Plotnikov et al., 2011). Interestingly, several groups reported that Nups are phosphorylated by ERK *in vivo* (Carlson et al., 2011; Kosako et al., 2009; Vomastek et al., 2008). Furthermore, it has been reported that ERK-mediated phosphorylation of FG Nups affects the nuclear translocation of importin-β (Kosako et al., 2009). These observations indicate a role of ERK in regulation of nucleocytoplasmic translocation (Czubryt et al., 2000; Kosako et al., 2009), which may produce feedback regulation to ERK translocation, although the details remain unclear.

Thus, accumulating evidence suggests the complex nature of ERK nuclear translocation. Here, I report that the nuclear translocation behaves like a switch in ERK signaling.

Overview

This dissertation consists of four main chapters, followed by Methods and References. Chapter 1 describes the concepts and essential backgrounds of the study. Specifically, I raise a question regarding a less intuitive behavior of ERK signaling system; that is, the output of the system defined by the level phosphorylation of ERK displays linear response, while ERK signaling regulates cell fate decision where sharp state transition should emerge. In Chapter 2, I provide evidence that nuclear translocation of ERK after growth factor-induced phosphorylation behaves like a switch. In addition, I show that the graded-to-switch-like conversion is observed in at least three different systems, i.e., EGF-stimulated PC12 cells, NGF-stimulated PC12 cells and

EGF-stimulated HeLa cells, confirming the generality of the phenomena. Chapter 3 will focus on the molecular mechanism that generates the switch-like response of nuclear translocation. First, I demonstrate that the conversion is dependent on ERK kinase activity, which indicates the existence of autoregulatory mechanisms involved in the switch-like response. Then, I investigate the contribution of ERK-mediated phosphorylation of nucleoporins to regulation of ERK nuclear translocation using *in vitro* reconstruction assay, mathematical modeling and knockdown experiments. In Chapter 4, I discuss the significance of the switch-like property of ERK signaling and concluding remarks are given.

Chapter 2: Nuclear translocation of ERK behaves like a switch

Graded response of EGF-induced ERK phosphorylation in PC12 cells

This study was performed to determine the response characteristics of ERK nuclear translocation and the underlying mechanisms that specify the shape of the response (Fig. 1) (Aoki et al., 2011). Epidermal growth factor (EGF) stimulation induces transient ERK phosphorylation and nuclear translocation in PC12 cells (Horgan and Stork, 2003). I first determined the dose–response relation in terms of ERK phosphorylation occurring in advance of nuclear translocation. Serum-starved cells were stimulated with various concentrations of EGF, and the levels of phosphorylated ERK were analyzed by Western blotting (Fig. 2a). The response data were fitted with the Hill function where the Hill coefficient (n_H) represents the degree of ultrasensitivity, giving $n_H = 1.2$ (Fig. 2b). The ratio of EC_{90} to EC_{10} (EC_{90}/EC_{10}) that is represented as $81^{(1/nH)}$ is useful to understand the degree of ultrasensitivity of the response (Ferrell and Ha, 2014a). The value of EC_{90}/EC_{10} was approximately 39 in the present study, indicating that a difference in input signal of more than an order of magnitude was required to switch the system from 10% to 90% maximal output. Therefore, ERK phosphorylation is induced in a graded manner in response to EGF stimulation. Note that the time courses of ERK phosphorylation in response to different EGF concentrations were similar except for the amplitude, suggesting that the result of the dose–response relation was less dependent on the time point at which the response was investigated (Fig. 2c).

The graded response observed by Western blotting may reflect a mixture of “on” and “off” cells at a single-cell level. To examine this possibility, I stimulated cells with high (50 ng ml^{-1} > EC_{90}),

intermediate (0.3 ng ml^{-1} ≈ EC_{50}) and low (0.01 ng ml^{-1} < EC_{10}) concentrations of EGF and analyzed the ERK phosphorylation in individual cells using immunofluorescence. If the graded response observed by Western blotting is due to a mixture of "on" and "off" cells, the histogram of the immunofluorescence intensity would be bimodal. The results confirmed that the distributions were unimodal rather than bimodal (Fig. 3), leading to rejection of the above suggestion. These results were also consistent with previous studies that examined EGF-induced ERK phosphorylation in single cells using immunofluorescence and flow cytometry (MacKeigan et al., 2005; Santos et al., 2007). Taken together, these observations indicated that EGF stimulation induced ERK phosphorylation in a graded manner.

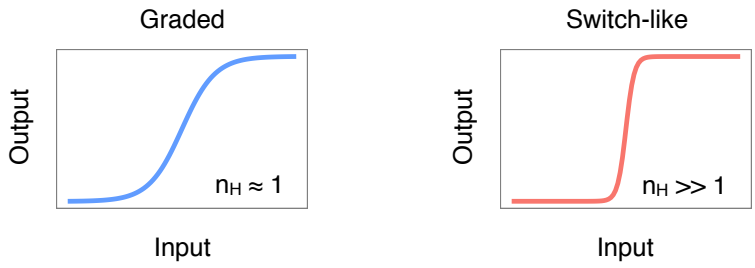

Figure 1: Schematic representation of the graded and switch-like responses of the system.

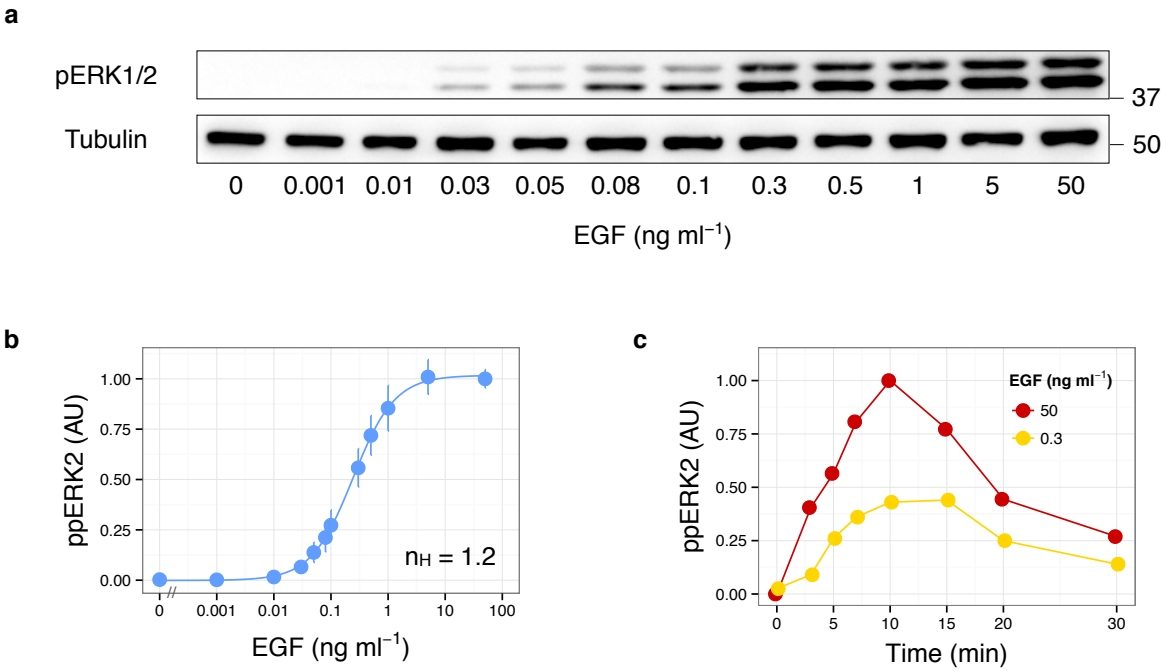

Figure 2: Graded response of EGF-induced ERK phosphorylation in PC12 cells.

(**a**) Serum-starved cells were stimulated with the indicated concentrations of EGF for 5 min, and the lysates were subjected to Western blotting analysis with anti-phospho ERK1/2. (**b**) The means of phosphorylated ERK2 intensity (AU) were plotted as a function of EGF concentration with standard errors of three independent experiments. The Hill coefficient was obtained by curve fitting with a Hill function. (**c**) Time courses of EGF-induced ERK phosphorylation. The lysates from EGF-treated (50 or 0.3 ng ml^{-1}) PC12 cells were subjected to Western blotting analysis with anti-phospho-ERK1/2 antibody at the indicated times.

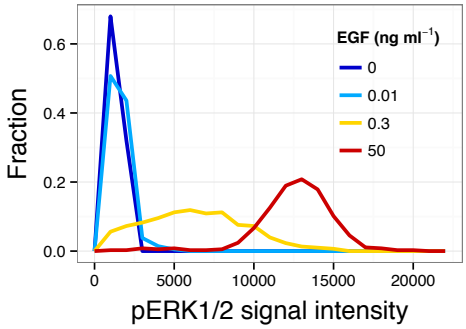

Figure 3: Distributions of ERK phosphorylation response.

Serum-starved cells were stimulated with the indicated concentrations of EGF for 5 min and then immunostained using anti-phospho ERK1/2 antibody. At least 100 cells were analyzed in each condition and histograms of fluorescence signals are shown.

Switch-like behavior of EGF-induced ERK nuclear translocation in PC12 cells

I then investigated the dose–response relation of ERK to EGF in terms of nuclear translocation. To visualize the stimulus-induced nuclear translocation of ERK in living cells, I constructed cells stably expressing GFP-ERK2 and histone H2B-mRFP1 as markers for ERK2 localization and the nucleus, respectively. Note that I used a clone expressing a low level of GFP-ERK2 compared to endogenous ERK (Fig. 4a) because overexpression of GFP-ERK2 sometimes causes abnormal ERK2 localization patterns (Costa et al., 2006). I also confirmed that there were no differences in the dynamics or dose–response of EGF-induced phosphorylation between GFP-ERK2 and authentic ERK (Fig. 4b, c). Upon EGF stimulation, transient GFP-ERK2 translocation was observed at the single-cell level (Fig. 4d). I also confirmed that the translocation was blocked by inhibition of MEK, a kinase of ERK, indicating that nuclear translocation requires ERK phosphorylation (Fig. 5).

Then, I stimulated cells with various concentrations of EGF and examined the cellular localization of GFP-ERK2 in thousands of living single cells to investigate the dose–response relation of ERK nuclear translocation to EGF stimulation (Fig. 6a, b). To measure the increase in nuclear GFP-ERK2 concentration in individual cells, the intensity of GFP-ERK2 in the nucleus was normalized relative to the value before stimulation (Cohen-Saidon et al., 2009), and the dose–response relation was determined. Surprisingly, I found that the response of nuclear translocation was much steeper than that of phosphorylation (Fig. 6c). The response was well fitted by a Hill function with $n_H = 4.2$ ($EC_{90}/EC_{10} = 2.8$), indicating that the “on” and “off” states of the system can be switched by approximately threefold differences in input signal. Taken

together, these results indicated that ERK nuclear translocation is induced in a switch-like manner.

I further analyzed the responses in individual cells. Upon stimulation with an apparent EC_{50} (~0.05 ng ml^{-1}) of EGF, individual cells typically did not show a "half" response but showed an "all-or-none" response (Fig. 7a). Indeed, the distribution of nuclear GFP-ERK2 intensity in single cells after EGF stimulation seemed to be bimodal (Fig. 7b). For quantitative assessment of the distribution, I calculated the mutual information between EGF and ERK nuclear translocation. In the context of input–output relation in cellular signaling, the mutual information indicates how many different input states are distinguishable according to a certain output value, or how many output values can be adopted by the input (Cheong et al., 2011). Here, the mutual information was approximately 1 bit (Fig. 7c), suggesting that EGF induces at most two distinct modes of ERK nuclear translocation response in a single cell.

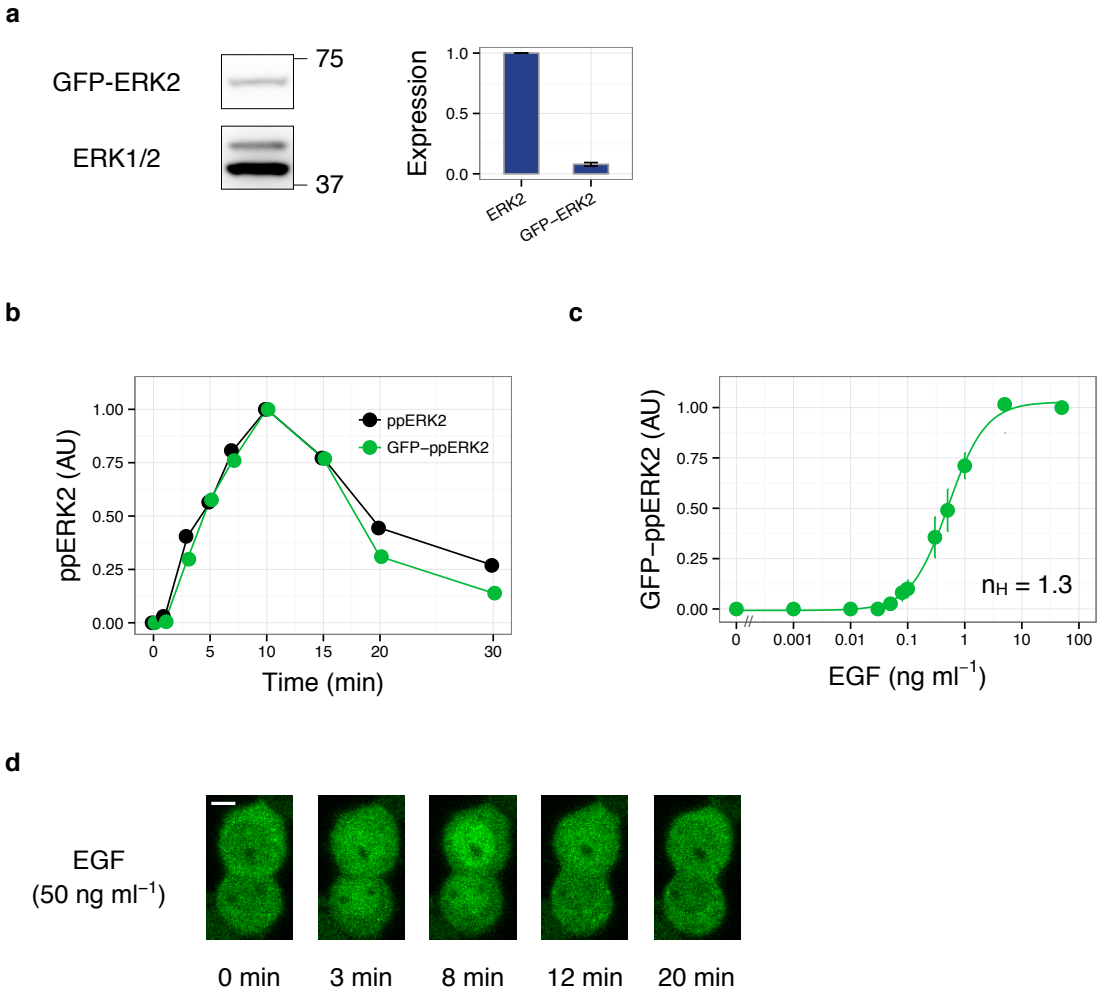

Figure 4: Live cell imaging of intracellular distributions of GFP-ERK2 in PC12 cells.

(**a**) The lysate from PC12 cells stably expressing GFP-ERK2 was subjected to Western blotting analysis with anti-ERK antibody. The expression level of GFP-ERK2 was much lower than that of endogenous ERK2, which is important to ensure few artifacts in the behavior or cellular localization of ERK. Error bars represent standard errors of three independent experiments. (**b**) Time course of EGF-induced (50 ng ml^{-1}) phosphorylation of exogenous GFP-ERK2 and endogenous ERK2. (**c**) The levels of GFP-ERK2 phosphorylation (AU) were plotted as a function of EGF concentration with standard errors of three independent experiments. Hill coefficient was obtained by curve fitting with a Hill function. (**d**) Time-lapse images of EGF-induced (50 ng ml^{-1}) GFP-ERK2 nuclear translocation as observed by live-cell imaging using a confocal microscope. Scale bar, 5 μm.

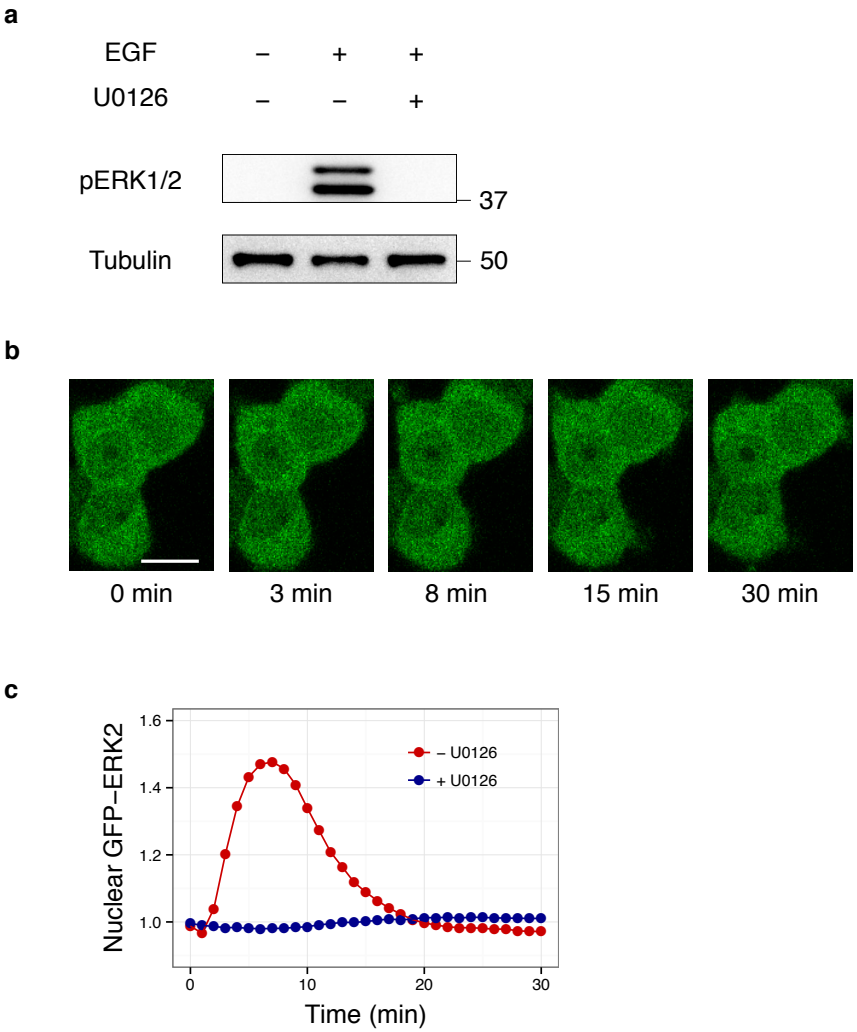

Figure 5: U0126 inhibits ERK phosphorylation and nuclear translocation.

(**a**) PC12 cells were treated with 10 µM U0126 or DMSO for 30 min and subsequently stimulated with EGF (50 ng ml^{-1}). The lysates were analyzed by Western blotting with anti-phospho- ERK1/2 antibody. (**b**) U0126-treated PC12 cells stably expressing GFP-ERK2 were stimulated with EGF (50 ng ml^{-1}) and time-lapse images were obtained at a time resolution of 1 min. Scale bar, 10 µm. (**c**) Time courses of mean nuclear GFP-ERK2 intensities (fold change) in U0126-treated (410 cells) or non-treated cells (220 cells).

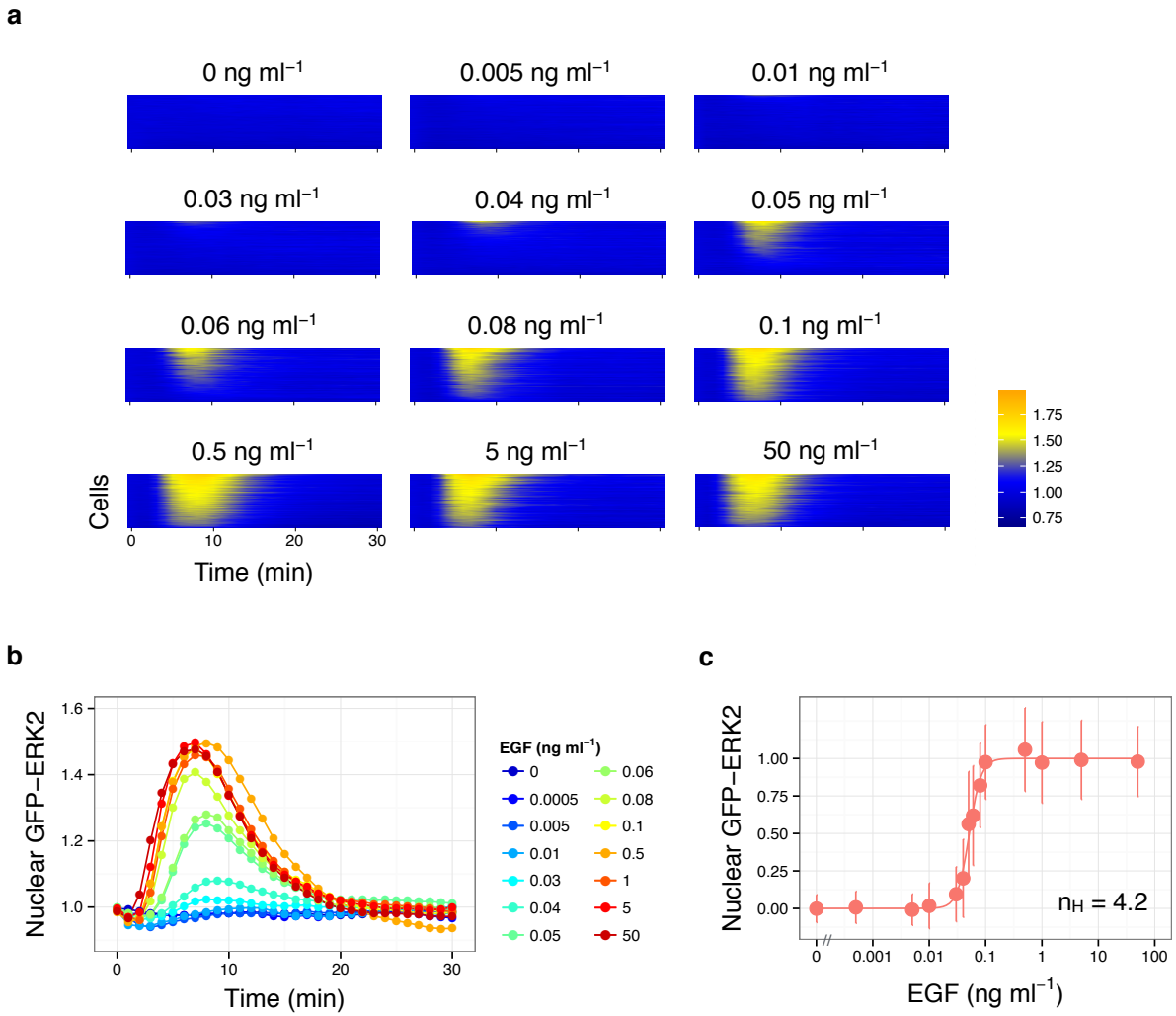

Figure 6: Switch-like response of EGF-induced ERK nuclear translocation.

(**a**) Cells were stimulated with the indicated concentration of EGF and time-lapse images were obtained at a time resolution of 1 min. At least 180 cells were observed in each condition and data for single cells (*y*-axis) are shown in the figures. Nuclear intensities of GFP-ERK2 were normalized by the value before stimulation to obtain the fold change increase in nuclear ERK2 concentration. (**b**) Averages of nuclear GFP-ERK2 intensities (fold change) in response to stimulation with the indicated concentrations of EGF. (**c**) The levels of nuclear GFP-ERK2 at 8 min after stimulation are shown as a function of EGF concentration with standard deviations. At least 180 cells were observed in each condition. Hill coefficient was obtained by curve fitting with a Hill function.

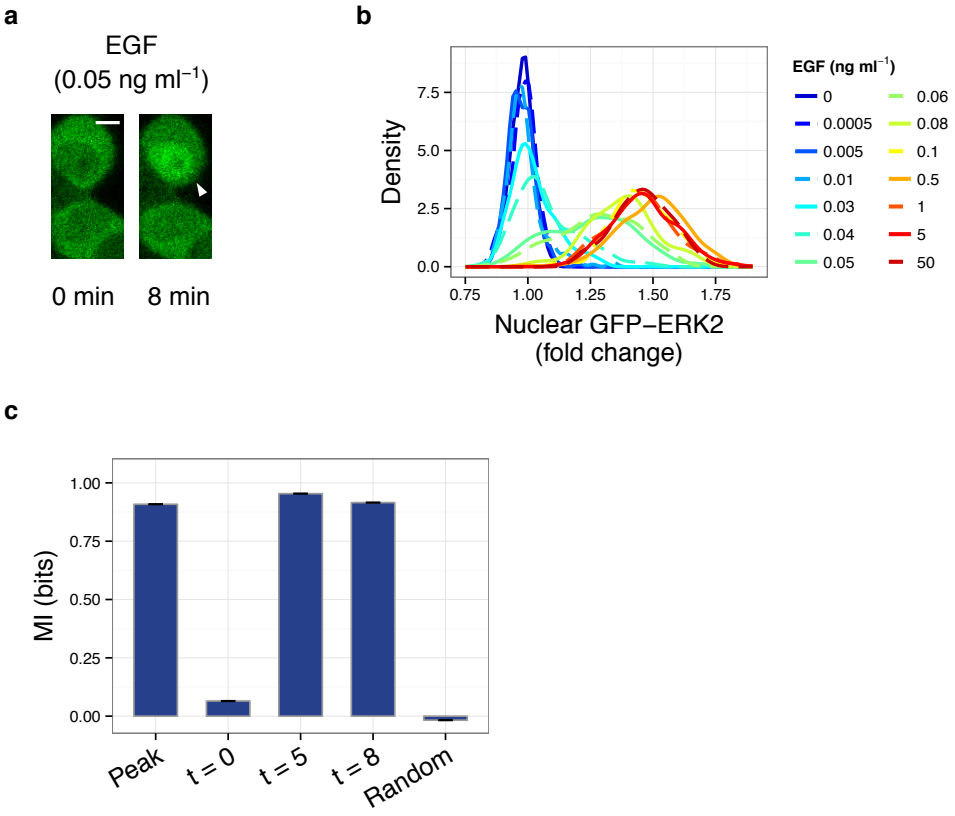

Figure 7: EGF-induced nuclear translocation response of ERK in individual cells.

(**a**) Nuclear translocation of GFP-ERK2 was induced in an all-or-none manner (white arrow) among individual cells upon stimulation with 0.05 ng ml^{-1} of EGF. Scale bar, 5 µm. (**b**) Distributions of nuclear GFP-ERK2 intensities (fold change) at 8 min after EGF stimulation. (**c**) Mutual information of nuclear GFP-ERK2 and EGF concentration.

The graded to switch-like conversion is a general property

I then tested the ERK response in two additional systems, i.e., nerve growth factor (NGF) stimulation in PC12 cells and EGF stimulation in HeLa cells, to examine the generality of the graded to switch-like conversion. NGF is known to induce neuronal differentiation in PC12 cells through activation of ERK signaling (Vaudry et al., 2002). In response to NGF stimulation, ERK shows transient and then sustained activation where the initial dynamics are similar to those induced by EGF (Fig. 8). Here, I focused on the NGF-induced initial activation of ERK and analyzed the dose–response relation. As with previous experiments, I stimulated cells with various concentrations of NGF, and analyzed the ERK response in terms of phosphorylation and nuclear translocation. The results indicated that NGF also induces ERK phosphorylation and nuclear translocation in graded (n_H = 1.2, EC_{90}/EC_{10} = 39) and switch-like (n_H = 4.1, EC_{90}/EC_{10} = 2.9) manners, respectively (Fig. 9).

Although I monitored the nuclear translocation of ERK using live cell imaging with an exogenous GFP-ERK2 probe, it would be informative to also test endogenous ERK behaviors. Therefore, the EGF-induced ERK response was investigated using immunofluorescence with anti-human ERK1, anti-ERK2 and anti-phospho-ERK1/2 antibodies in HeLa cells. Anti-human ERK1 and anti-ERK2 antibodies were not cross-reactive with ERK2 and ERK1, respectively (Fig. 10), which allowed analyses of ERK nuclear translocation response at the level of the isoform. Serum-starved HeLa cells were stimulated with various concentrations of EGF and analyzed ERK phosphorylation and nuclear translocation (Fig. 11). As observed in PC12 cells, I confirmed that the phosphorylation was induced in a graded manner (n_H = 1.5, EC_{90}/EC_{10} = 19) even in HeLa

cells (Fig. 12, blue). On the other hand, immunofluorescence of anti-human ERK1 and anti-ERK2 antibodies clearly indicated that the nuclear translocation in response to EGF was induced in a switch-like manner (n_H = 4.0, EC_{90}/EC_{10} = 3.0) in HeLa cells (Fig. 12, red).

Thus, I confirmed that graded phosphorylation is converted into switch-like nuclear translocation in at least three different systems, i.e., EGF-stimulated PC12 cells, NGF-stimulated PC12 cells and EGF-stimulated HeLa cells. These results indicate that the conversion of graded phosphorylation into switch-like nuclear translocation is a general property of growth factor-induced ERK signaling. Note that the EC_{50} concentration of growth factors for ERK nuclear translocation response was smaller than that for the ERK phosphorylation response, which was observed in all systems examined (Table 1). Therefore, the process of nuclear translocation increases in both steepness of the response (n_H) and sensitivity to the signal input (EC_{50}).

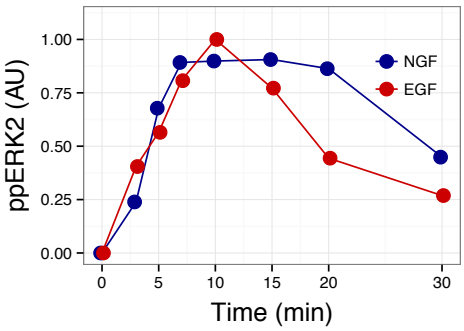

Figure 8: Time courses of EGF or NGF-induced ERK phosphorylation.

The lysates from NGF-treated (50 ng ml^{-1}) PC12 cells were analyzed by Western blotting with anti-phospho-ERK1/2 antibody at the indicated times, and shown with the time course induced by 50 ng ml^{-1} EGF.

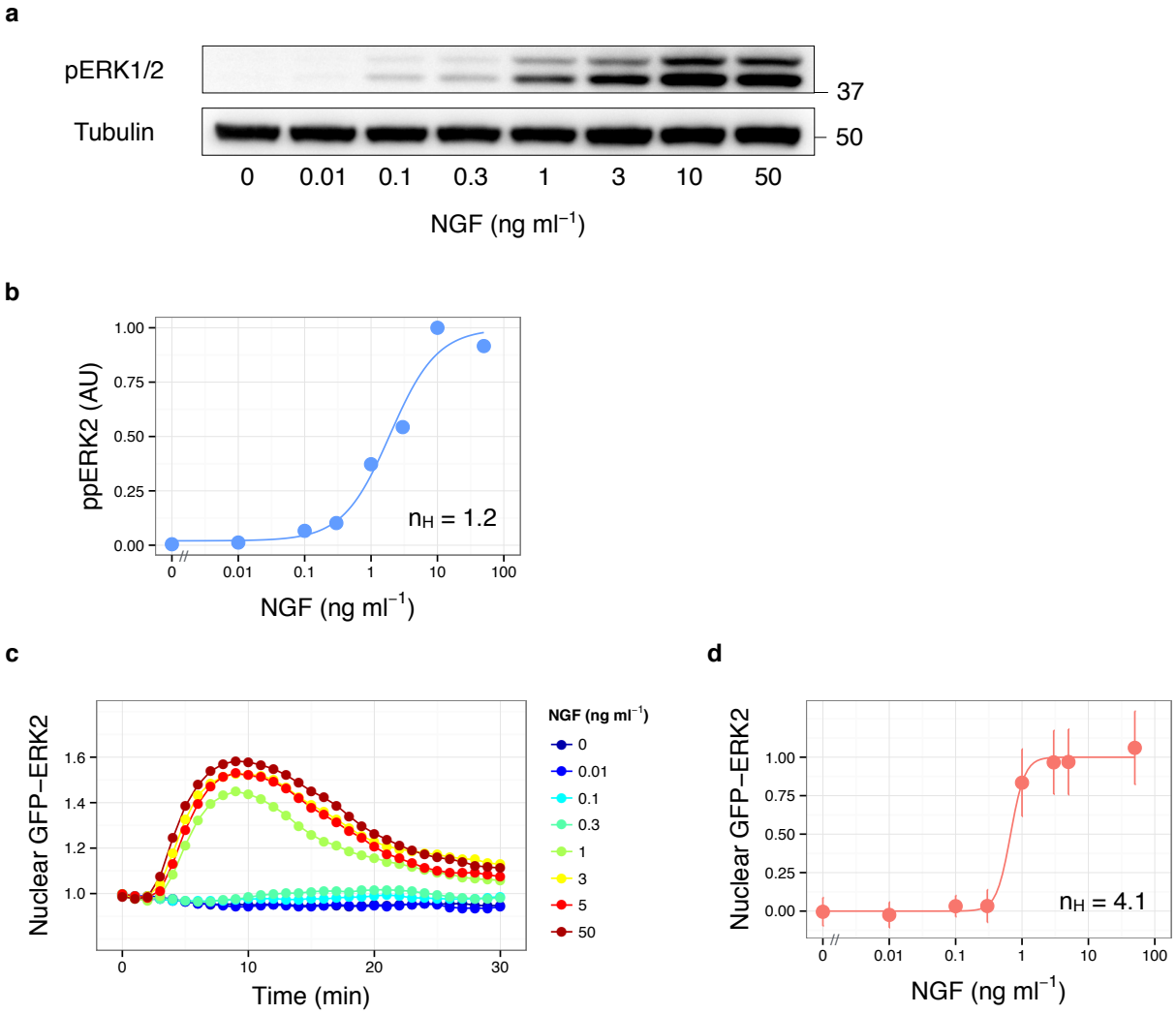

Figure 9: ERK behavior in response to NGF stimulation in PC12 cells.

(**a**) Serum-starved PC12 cells were stimulated with the indicated concentrations of NGF for 5 min, and the lysates were subjected to Western blotting analysis with anti-phospho-ERK1/2 antibody. (**b**) The levels of phosphorylated ERK2 (AU) were plotted as a function of NGF concentration. (**c**) Averages of nuclear GFP-ERK2 intensities (fold change) in response to stimulation with the indicated concentrations of NGF. (**d**) The levels of nuclear GFP-ERK2 at 9 min after stimulation are shown as a function of NGF concentration with standard deviations. At least 148 cells were observed in each condition. The Hill coefficient was obtained by curve fitting with a Hill function.

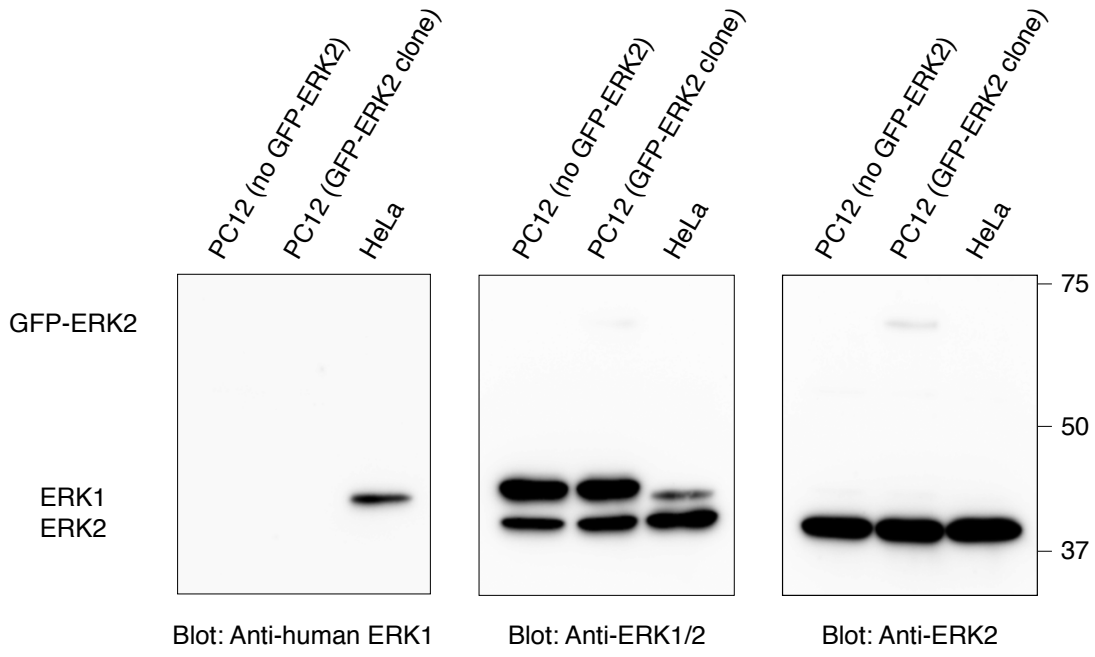

Figure 10: Confirmation of the specificity of anti-human ERK1 and anti-ERK2 antibodies.

The lysates from PC12 cells, PC12 cells stably expressing GFP-ERK2, and HeLa cells were subjected to Western blotting analysis with anti-human ERK1 antibody (left), anti-ERK1/2 antibody (middle) and anti-ERK2 antibody (right). Note that no anti-human ERK1 signal was observed in the lysate from PC12 cells derived from rats.

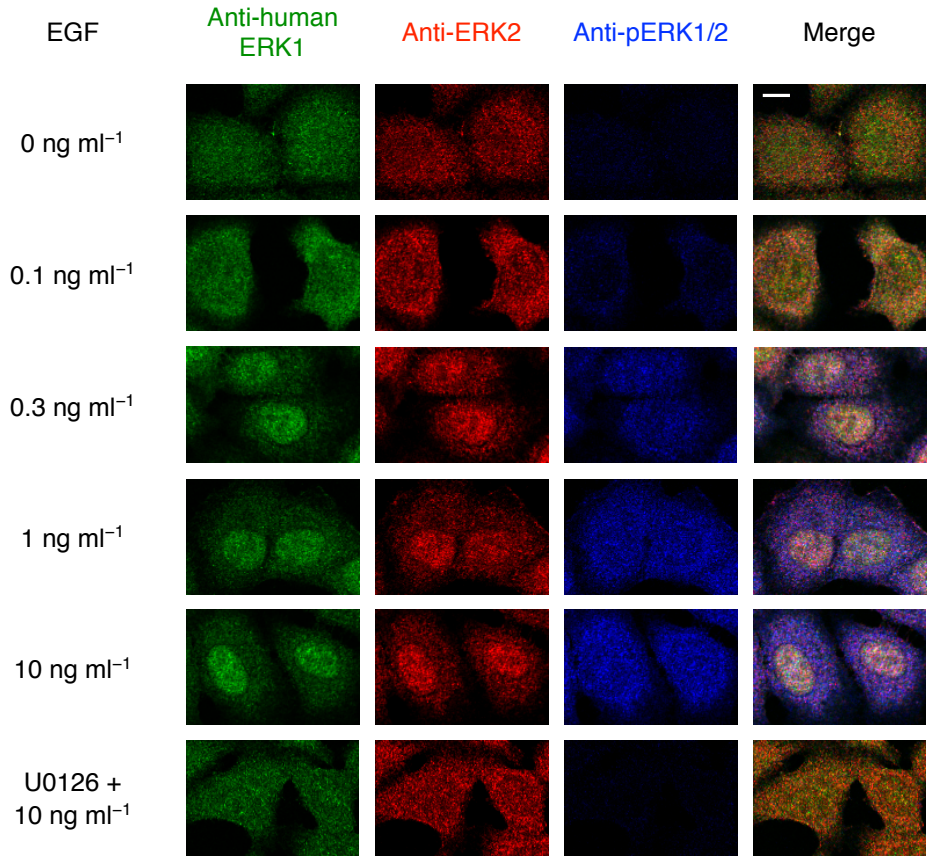

Figure 11: Immunofluorescence of ERK1, ERK2 and pERK1/2 in HeLa cells.

Serum-starved HeLa cells were stimulated with the indicated concentrations of EGF for 10 min, and triply immunostained with anti-human ERK1, anti-ERK2 and anti-phospho-ERK1/2 antibodies. Scale bar, 10 μm.

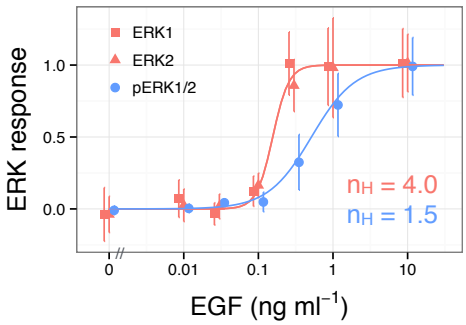

Figure 12: EGF-induced ERK response in HeLa cells.

The levels of ERK1/2 phosphorylation (blue) and nuclear/cytoplasmic ratio of ERK1 and ERK2 (red) were plotted as a function of EGF concentration with standard deviations. At least 100 cells were observed in each condition. The Hill coefficients were obtained by curve fitting with a Hill function.

Table 1: EC_{50} concentrations of growth factors for ERK response.

Stimulation / Cells	EC50 (phosphorylation)	EC50 (nuclear translocation)
EGF / PC12	0.2 ng ml^{-1}	0.05 ng ml^{-1}
NGF / PC12	2 ng ml^{-1}	0.7 ng ml^{-1}
EGF / HeLa	0.5 ng ml^{-1}	0.2 ng ml^{-1}

Chapter 3: Molecular mechanism of the graded-to-switch-like conversion

ERK kinase activity is involved in the switch-like nuclear translocation response

As ERK phosphorylation showed a graded response, whereas nuclear translocation showed a switch-like response, there should be some mechanism(s) for the conversion from a graded to a switch-like response. Although there are several possible mechanisms to generate ultrasensitive responses, one of the most commonly observed is an autoregulatory mechanism that is dependent on its own activity (Fig. 13a). Therefore, I examined whether the switch-like behavior of nuclear translocation was dependent on ERK activity using the ERK inhibitor FR180204 (Ohori et al., 2005). Treatment of cells with the ERK inhibitor was confirmed to extensively block the phosphorylation of p90RSK, which is one of the major substrates of ERK (Fig. 13b). Note that the dynamic property of ERK phosphorylation after 10 min was changed by the ERK inhibitor, which showed sustained dynamics for at least 30 min after stimulation (Fig. 14a). This was probably due to inhibition of negative feedback from ERK to the upstream of ERK (Kamioka et al., 2010). Nevertheless, the response of ERK phosphorylation was still graded (n_H = 1.4, EC_{90}/EC_{10} = 23) even in ERK inhibitor-treated cells (Fig. 14b). In contrast, ERK nuclear translocation showed a graded rather than switch-like response (n_H = 1.2, EC_{90}/EC_{10} = 39) in ERK inhibitor-treated cells (Fig. 14c, d). Nuclear translocation also showed sustained dynamics similar to phosphorylation, and the initial slope of nuclear import and the level of nuclear accumulation were proportional to the EGF concentration (Fig. 14c). These findings strongly suggested that ERK activity plays a significant role in the switch-like nuclear translocation response. That is, the switch-like response of ERK nuclear translocation is achieved by autoregulatory mechanisms.

Figure 13: Possible relationship between ERK activity and nuclear translocation.

(**a**) Schematic representation of possible relationship between ERK activity and nuclear translocation. (**b**) PC12 cells were treated with FR180204 or DMSO and subsequently stimulated with EGF (50 ng ml^{-1}) for 10 min. The lysates were subjected to Western blotting analysis with the indicated antibodies.

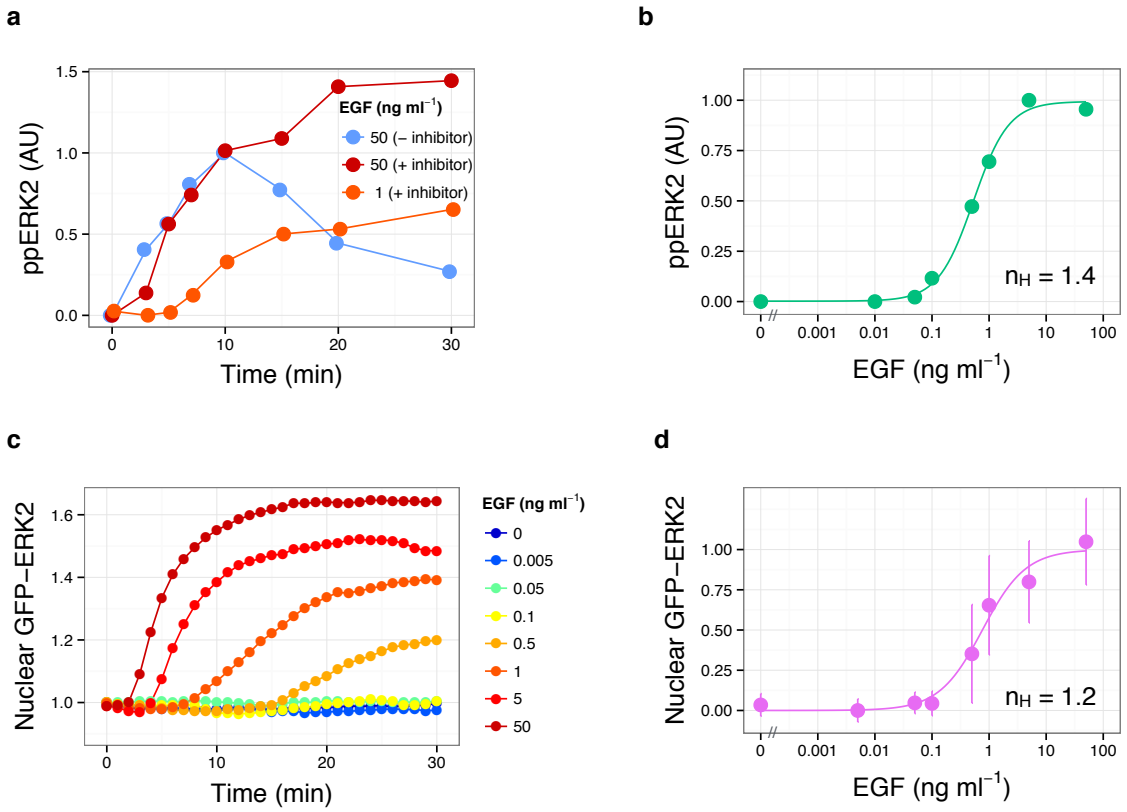

Figure 14: Switch-like nuclear translocation is dependent on ERK kinase activity.

(**a**) Time courses of ERK2 phosphorylation (AU) induced by EGF stimulation in ERK inhibitor-treated or non-treated PC12 cells. (**b**) The levels of phosphorylated ERK2 (AU) at 30 min after EGF stimulation in ERK inhibitor-treated cells were plotted as a function of EGF concentration. The Hill coefficient was obtained by curve fitting with a Hill function. (**c**) Cells were treated with ERK inhibitor and stimulated with the indicated concentrations of EGF, and the time courses of nuclear GFP-ERK2 intensities (fold change) are shown. (**d**) The levels of nuclear GFP-ERK2 at 30 min after stimulation in ERK inhibitor-treated cells are shown as a function of EGF concentration with standard deviations. At least 132 cells were observed in each condition. The Hill coefficient was obtained by curve fitting with a Hill function.

ERK-mediated phosphorylation of Nups regulates ERK nuclear translocation

The above results with ERK inhibitors raised questions regarding the link between ERK activity and nuclear translocation regulation. Among ERK substrates reported to date (Yoon and Seger, 2006), NPC proteins including FG Nups are related to nucleocytoplasmic translocation. Indeed, it has been reported that ERK-mediated phosphorylation of FG Nups affects the nuclear translocation of importin-β (Kosako et al., 2009). Therefore, one possible scenario for the link between ERK activity and ERK nuclear translocation is that ERK regulates the NPC environment through phosphorylation, which leads to changes in the kinetics of ERK nuclear translocation. To validate this hypothesis, I reconstructed ERK nuclear translocation in digitonin-permeabilized cells. Prior to the import assay, I incubated digitonin-permeabilized cells with recombinant GFP-ppERK2 (Fig. 15a) to induce ERK-mediated phosphorylation of Nups. I confirmed that at least four of the FG Nups known as ERK substrates (Carlson et al., 2011; Kosako et al., 2009), i.e., Nup214, Nup153, Nup62 and Nup50, were phosphorylated in digitonin-permeabilized cells (Fig. 15b, c). After washing cells with transport buffer, I examined time-lapse images of GFP-ppERK2 nuclear translocation (Fig. 16a). The results showed that GFP-ppERK2 entered the nucleus faster in cells that were pre-incubated with GFP-ppERK2 than in those pre-incubated with GFP or GFP-ppERK2 plus ERK inhibitor (Fig. 16b). For example, the nuclear intensity at 20 s was significantly higher in GFP-ppERK2-treated cells ($P < 0.05$; *t* test). The steady-state level (~120 s) was not significantly different ($P > 0.05$; *t* test), indicating that the effect was bidirectional. Therefore, I found that the ERK-mediated phosphorylation of Nups accelerates nucleocytoplasmic translocation of ERK. This was in contrast with the case of importin-β, the

nuclear import of which was reduced, indicating that ERK-mediated phosphorylation of Nups can both up- and downregulate nucleocytoplasmic translocation. Taken together, these observations indicated that ERK nuclear translocation was enhanced by ERK-mediated phosphorylation of Nups, which is one of the molecular mechanisms involved in autoregulation of ERK nuclear translocation (Fig. 16c). Note that the translocation in this assay was carrier-independent because the assay was performed with digitonin-permeabilized cells that lacked cytoplasmic factors. Similarly, there was no cytoplasmic sequestration of ERK by anchor proteins, and therefore the apparent rate of nuclear translocation in the assay was fast compared to the timescale of the stimulus-induced nuclear translocation of ERK in living cells.

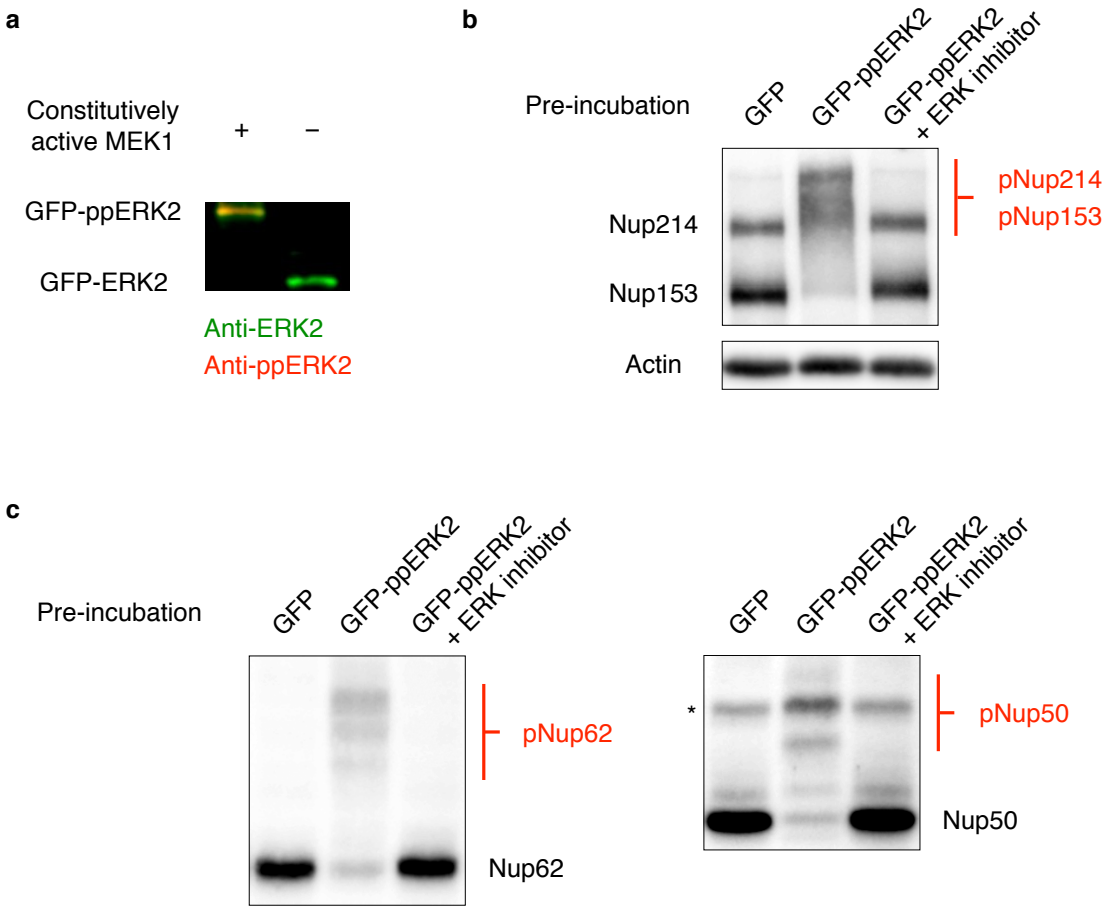

Figure 15: *In vitro* phosphorylation of nucleoporins (Nups) in digitonin-permeabilized cells.

(**a**) Purification of GFP-ppERK2. *E. coli* was co-transformed with plasmids of GFP-ERK2 and constitutively active MEK1 to obtain phospho-form of GFP-ERK2. Phosphorylation was confirmed by Mn^{2+}-Phos-tag SDS-PAGE, followed by immunoblotting with anti-ERK mouse antibody and Alexa Fluor 488-conjugated anti-mouse IgG antibody as a secondary antibody, anti-ppERK2 rabbit antibody and Alexa Fluor 647-conjugated anti-rabbit IgG antibody as a secondary antibody. (**b, c**) Digitonin-permeabilized cells were pre-incubated with GFP-ppERK2 or GFP (negative control), with ERK inhibitor or DMSO to induce ERK-mediated phosphorylation of Nups. Phosphorylation was confirmed by Mn^{2+}-Phos-tag Western blotting analysis. The asterisk indicates non-specific bands.

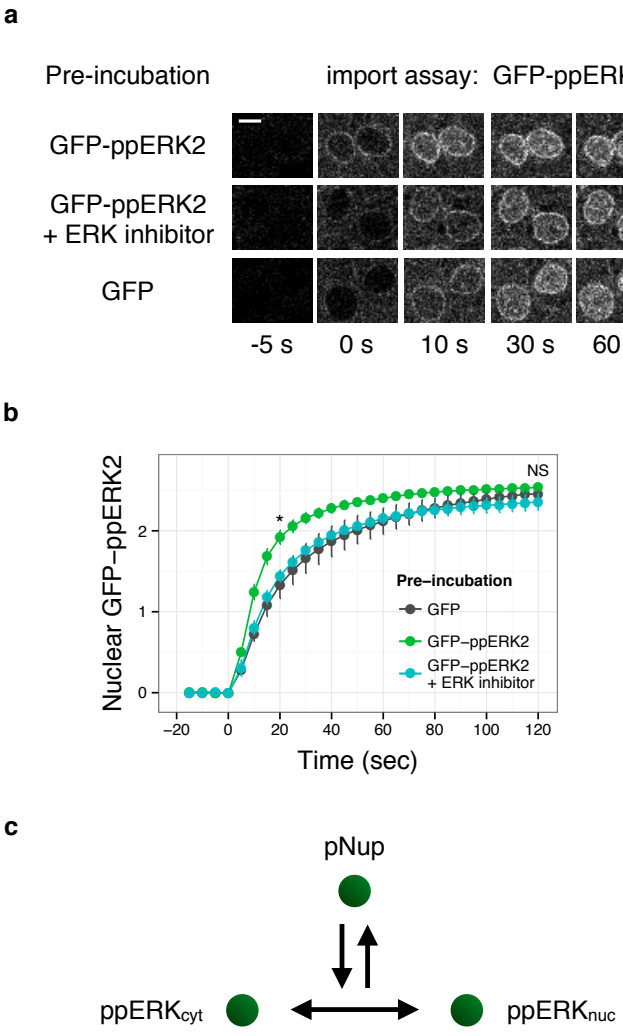

Figure 16: ERK-mediated phosphorylation of Nups enhances ERK nuclear translocation.

(**a**) Nuclear import of GFP-ppERK2 was observed in digitonin-permeabilized cells at a time resolution of 5 s. Scale bar, 5 μm. (**b**) Time courses of GFP-ppERK2 nuclear import were quantified and shown with standard errors of three independent experiments. Student's *t* test was used to analyze the data at 20 s and 120 s. **P* < 0.05, NS = not significant. (**c**) Schematic representation of nuclear translocation regulation via ERK-mediated phosphorylation of Nups.

Kinetic modeling of ERK nuclear translocation

The results outlined above are strongly suggestive of a link between ERK activity and ERK nuclear translocation; however, it is not clear whether the ERK-mediated regulation of its own nuclear translocation is adequate to reproduce experimentally observed data, including the conversion from a graded to a switch-like ERK response. To investigate this question, I constructed an ordinary differential equation model of ERK phosphorylation and nuclear translocation accompanied with translocation regulation via Nups. The basic structure of the model was derived from the previous study, which explained the time courses of both phosphorylation and nuclear translocation (Ahmed et al., 2014). The model was updated by integrating the results of ERK-mediated Nup phosphorylation and translocation regulation (Fig. 17). The model is described in the following scheme.

1) A transient input signal is induced in a stimulus-dependent manner and initiates the phosphorylation of cytoplasmic ERK.
2) Cytoplasmic ppERK suppresses the input signals (negative feedback to Sos)
3) ERK and ppERK undergo nucleocytoplasmic shuttling.
4) Nup is phosphorylated by ppERK in proportion to the rate of nucleocytoplasmic shutting of ppERK.
5) Nuclear ppERK binds nuclear substrates and catalyzes phosphorylation.
6) Phosphorylated ERK, Nup and substrates are dephosphorylated.

The model did not explicitly include active transport for several reasons as follows. 1) ERK can enter the nucleus without transport carriers or energy (Matsubayashi et al., 2001; Whitehurst et al.,

2002). 2) Active transport of ERK presumably requires dimerization, but the rate of transport does not seem to be different between the wild-type and dimerization-deficient mutant in living cells (Lidke et al., 2010). 3) The nuclear translocation model with active transport does not improve the fit to the data (Ahmed et al., 2014). For the process of ERK-mediated phosphorylation of Nup, I assumed that ppERK both entering and exiting the nucleus is able to catalyze phosphorylation. Furthermore, the probability that Nup encounters ppERK is expected to be proportional to the amount of ppERK that passes through the nucleus per unit time rather than the concentration of cytoplasmic or nuclear ppERK. Therefore, in the model, the rate of Nup phosphorylation was proportional to the rate of ppERK translocation.

Then, the model parameters were fitted to the experimental data by optimization (Materials and Methods). Consequently, the model well reproduced the time course of both ERK phosphorylation and nuclear translocation (Fig. 18a, b). In addition, the model successfully realized conversion of graded phosphorylation into switch-like nuclear translocation (Fig. 18c, d). Note that I could not reproduce the observed data by the model without Nups. To understand the processes responsible for the switch-like response, I calculated sensitivity coefficients for the Hill coefficient of ERK nuclear translocation response by making 1% changes in model parameters. The results indicated that not only parameters that were directly related to nuclear ERK but also those related to Nups showed large sensitivity coefficients (Fig. 19). These results strongly suggest a significant role of the newly introduced processes, autoregulatory mechanisms for ERK translocation in the conversion from a graded to a switch-like ERK response.

At an early stage after stimulation, ERK is phosphorylated in the cytoplasm. Activated ERK passes across the nuclear envelope with phosphorylation of Nups and interacts with nuclear

substrates, resulting in accumulation of ERK in the nucleus. ERK-mediated phosphorylation of Nups enhances ERK import, which works as positive feedback on nuclear import. On the other hand, the nuclear accumulation of ERK does not last long because the available substrates would be decreased by phosphorylation (Ahmed et al., 2014), which functions as negative feedback for ERK nuclear import. Therefore, both positive and negative feedback regulations temporarily emerge. Indeed, positive and negative feedback is a motif observed in excitable systems that is known to inherently generate ultrasensitive responses (Alon, 2007; Pomerening et al., 2003). Therefore, the ERK model could be interpreted as a modified form of the excitable system.

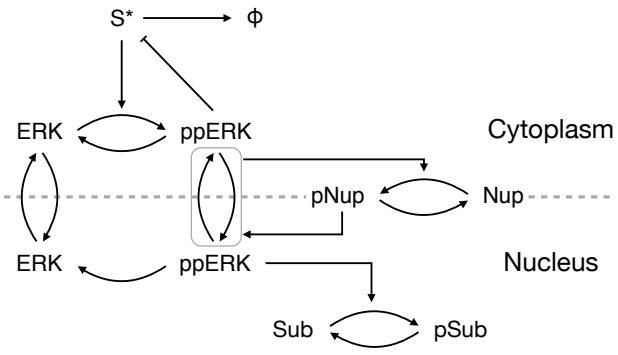

Figure 17: Topology scheme of the model.

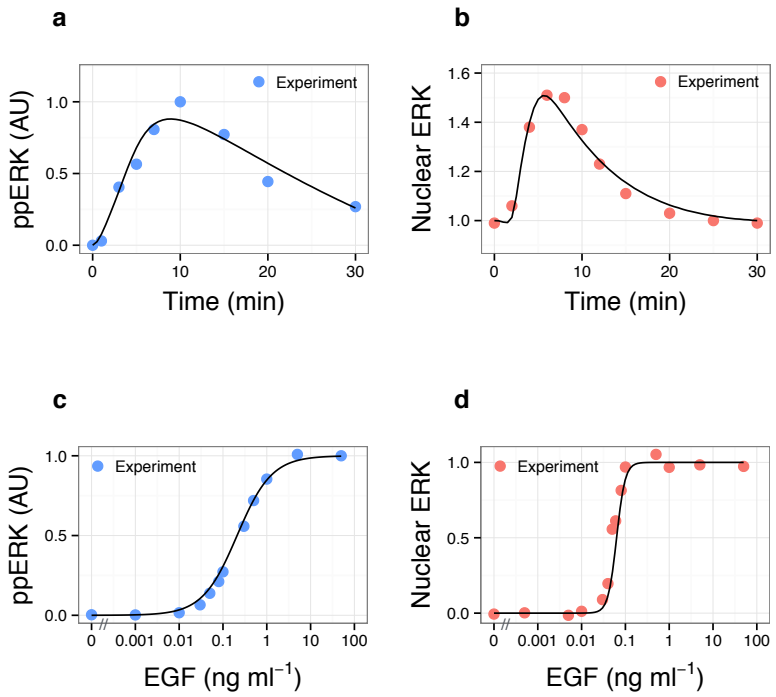

Figure 18: The model reproduced the experimental data.

(**a**) Time courses of ppERK and (**b**) nuclear ERK in response to EGF (50 ng ml^{-1}) stimulation were numerically simulated with the model (solid lines). Points represent experimental data. (**c**) Dose–response relation of EGF and ppERK or (**d**) nuclear ERK. Points and solid lines indicate experimental and simulation data, respectively.

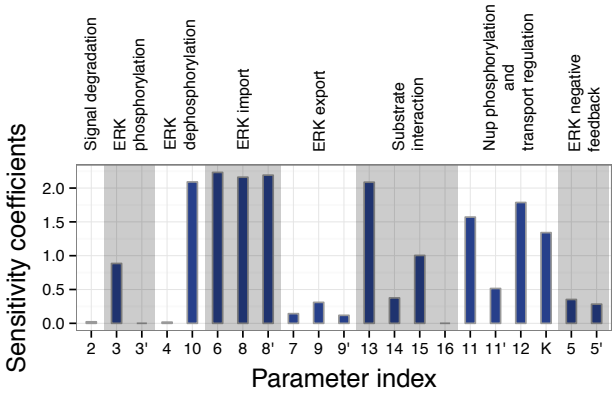

Figure 19: Sensitivity analysis for the Hill coefficient of ERK nuclear translocation response.

Sensitivity coefficients were calculated by making 1% changes in parameters and absolute values are shown.

Depletion of Nup153 affects the ERK nuclear translocation

The results of *in vitro* and *in silico* analyses in the present study suggested a correlation between Nup phosphorylation and ERK nuclear translocation. However, it remains unclear if Nups modulate ERK behaviors in living cells. Therefore, I investigated ERK nuclear translocation with depletion of Nup153 (Fig. 20a), one of the relevant Nups that is most effectively phosphorylated by ERK (Kosako et al., 2009). Knockdown of Nup153 did not cause any abnormal ERK2 localization patterns before stimulation (Fig. 20b, $P > 0.05$; *t* test). As with previous experiments, cells were stimulated with various concentrations of EGF and the nuclear translocation response of GFP-ERK2 was investigated (Fig. 20c). The results indicated that the steepness of the EGF-induced ERK nuclear translocation response was more gradual in Nup153-depleted cells than in non-depleted cells (Fig. 20d), suggesting a contribution of Nup153 to regulation of the ERK nuclear translocation response.

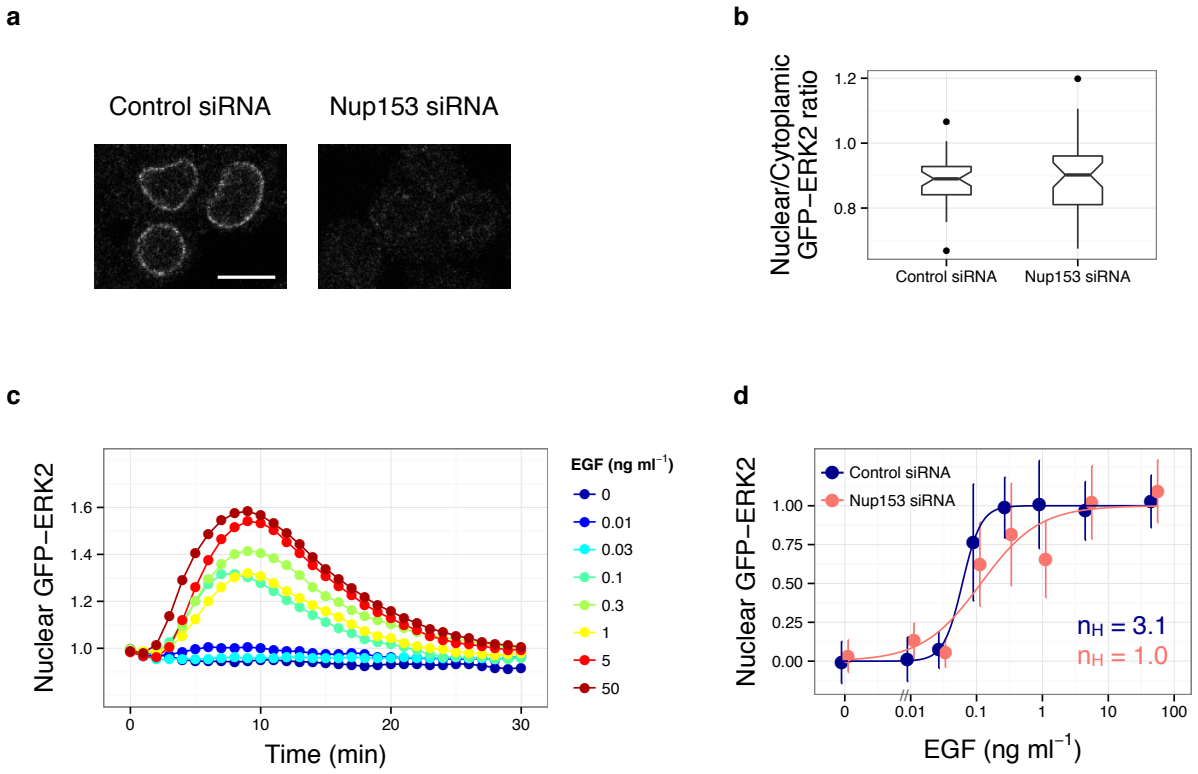

Figure 20: Depletion of Nup153 affects the ERK nuclear translocation response.

(**a**) Cells were transfected with Nup153 siRNA or control siRNA duplexes, and immunostained with anti-Nup153 antibody at 64 h after transfection. Scale bar, 10 μm. (**b**) The distributions of nuclear/cytoplasmic ratio of GFP-ERK2 in Nup153-depleted or non-depleted cells are shown as box plots. No significant differences were observed ($P > 0.05$; *t* test). (**c**) Time courses of mean nuclear GFP-ERK2 intensities (fold change) in Nup153-depleted cells. Cells were stimulated with the indicated concentrations of EGF at 64 h after Nup153 siRNA transfection. Immediately after the live imaging experiments, cells were fixed, immunostained with anti-Nup153 antibody and the Nup153-depleted cells were used for the analyses. At least 34 cells from four independent fields of view were analyzed in each condition. (**d**) The levels of nuclear GFP-ERK2 at 9 min after stimulation in Nup153-depleted or non-depleted cells are shown as a function of EGF concentration with standard deviations. The Hill coefficient was obtained by curve fitting with a Hill function.

Chapter 4: Discussion

ERK MAP kinase signaling is an important master regulator of the cell fate decision in various mammalian cells. This system was therefore expected to behave like a switch, while the output of the system defined by the amount of phosphorylation of ERK has been shown to display a linear response, which raises questions regarding how such a linear system can produce completely different cell fates in individual cells. Here, I presented evidence that, rather than phosphorylation itself, subsequent nuclear translocation accompanied by autoregulatory mechanisms acts as a switch in ERK signaling.

Significance of the switch-like behavior in ERK signaling

The ultrasensitive switch-like response of ERK signaling could be significant for several reasons. First, switch-like behavior that filters out noise or markedly low-level extracellular signals could be important to avoid erroneous responses. Otherwise, ERK would be induced even without extracellular signals, which would probably lead to various dysfunctions in cell physiology (Kim and Choi, 2010). Second, the ultrasensitivity of the system eliminates the ambiguity of the signal. This is reasonable as ERK regulates the cell fate decision, including proliferation, differentiation, survival and death, which are essentially all-or-none biological phenomena. Indeed, a pulse-like increase in ERK activity in the nucleus was observed using FRET biosensors in proliferating cells (Aoki et al., 2013). They also revealed that the frequency of the pulse, but not the amplitude, was significant for ERK-dependent cell proliferation. Therefore, the reduction of ambiguity in ERK

signaling would be reasonable for cells.

The switch-like nuclear translocation, but not phosphorylation, may enable different ERK activities in the cytoplasm and nucleus; i.e., cytoplasmic substrates would be phosphorylated in a graded manner, while phosphorylation of nuclear substrates would be regulated in a switch-like manner. Indeed, it has been reported that phosphorylation of RSK1, one of the major cytoplasmic targets of ERK, shows a graded response, while phosphorylation of c-Fos that is localized to the nucleus is more sensitive than that of RSK1 (MacKeigan et al., 2005), although the underlying mechanism was unclear. Thus, the non-linear property of ERK nuclear translocation may be the basis for the distinct ERK activities in each subcellular location. Consistent with this suggestion, regulation of ERK activity at the level of subcellular localization has recently been reported to be tightly associated with the cell fate decision in myogenesis where cytoplasmic and nuclear ERK induce differentiation and proliferation, respectively (Michailovici et al., 2014).

The regulation of nuclear translocation in ERK signaling could be understood in terms of the increase in sensitivity to growth factors because the EC_{50} for the nuclear translocation response was lower than that for phosphorylation (Table 1). That is, at most less than half-maximal level of ERK phosphorylation is sufficient to fully evoke stimulus-induced nuclear translocation. Recently, the relationship between ERK phosphorylation and cell proliferation was investigated quantitatively, and the results indicated that the basal level of ERK phosphorylation was ~10%, which reaches only ~30% even at the peak (Aoki et al., 2013). Therefore, cells use only 20% changes in the level of ERK phosphorylation under physiological conditions, but this would be sufficient to effectively transfer the extracellular information into the nucleus in a switch-like manner.

Other possible mechanisms involved in regulation to ERK nuclear translocation

In the present study, I proposed that ERK-mediated phosphorylation of Nups is one of the possible autoregulatory mechanisms. Although only a few proteins, including NPC proteins, are known as substrates of ERK that seem to be related directly to nucleocytoplasmic translocation, it remains possible that there are also other underlying mechanisms. As shown in the import assay as well as in previous studies, ERK is able to enter the nucleus without a carrier or energy. In contrast, a carrier-dependent pathway that depends on Imp7 has also been reported, which involves phosphorylation on the Ser residues at an SPS (Ser244, Pro245 and Ser246) motif in the kinase insert of ERK (Chuderland et al., 2008). The SPS motif lies within an ERK consensus phosphorylation site and Ser244 is indeed phosphorylated by ERK (Plotnikov et al., 2011). Therefore, the autophosphorylation may act as an autoregulatory mechanism for nuclear translocation of ERK, although Casein kinase 2 mostly mediates SPS phosphorylation *in vivo* (Plotnikov et al., 2011). In addition, the subcellular localization of ERK is regulated by cytoplasmic sequestration through interactions with several anchor proteins, such as MEK, Sef and PEA-15 (Formstecher et al., 2001; Fukuda et al., 1997; Torii et al., 2004). If the sequestration by the anchor proteins is under control of ERK activity, this would be another mechanism for the autoregulation of ERK translocation.

Concluding remarks

Non-linear behaviors, including ultrasensitivity, oscillation and bistability, are the basis of the higher-order function of biological systems. The complex nature of the ERK MAP kinase

phosphorylation cascade has been studied extensively, while subsequent nuclear translocation has often been neglected. Nevertheless, my study demonstrated that ERK phosphorylation is likely to show a mostly linear response, at least in mammalian cells, whereas nuclear translocation is a highly regulated process that behaves like a switch. Thus, my study shed light on the importance of not only the phosphorylation cascade but also nuclear translocation, which characterizes the system behavior in the ERK signaling pathway.

Methods

Preparation of plasmids, reagents and antibodies

The cDNA of human ERK2 was inserted into pEGFP-C2 vector with a monomeric A206K mutation (GFP-ERK2). A fragment of GFP-ERK2 was introduced into pGEX2T vector, and then an N-terminal PreScission site and C-terminal His_8 tag were introduced (pGEX-GFP-ERK2-His). The plasmids H2B-mRFP1 and pACYC184-Venus-MEK1 (S218/222E, Δ32-51) were prepared as described previously (Kanda et al., 1998; Kimura and Cook, 2001; Takahashi et al., 2012). EGF was purchased from PeproTech. The MEK inhibitor, U0126, was purchased from Promega. The ERK inhibitor, FR180204, was purchased from Santa Cruz. Phos-tag acrylamide was purchased from Wako. Digitonin was purchased from Calbiochem. Anti-ERK1/2 (L34F12 and 137F5), anti-phospho-ERK1/2 (E10 and D13.14.4E), anti-phospho-p90RSK (D3H11) and anti-alpha-tubulin (DM1A) antibodies were purchased from Cell Signaling Technology. Anti-human ERK1 (Y72) antibody was purchased from Abcam. Anti-ERK2 (D-2) antibody was purchased from Santa Cruz. Anti-actin IgM (clone JLA20) antibody was purchased from the Developmental Studies Hybridoma Bank. Anti-Nup153 (7A8) antibody was purchased from Progen. QE5 anti-Nup153 antibody that also recognizes Nup214 and Nup62 was purchased from Covance. Anti-Nup50 antibody was provided by Dr. H. Kosako (Tokushima University, Japan). The linearity of Western blotting analysis was confirmed by serial dilution of the lysates, followed by immunoblotting with anti-phospho-ERK1/2 antibody. Phos-tag Western blotting was performed in gels containing 7.5% acrylamide, 50 μM $MnCl_2$ and 25 μM Phos-tag, followed by immunoblotting.

Cell culture

Rat PC12 pheochromocytoma cells stably expressing GFP-ERK2 and H2B-mRFP1 were provided by Dr. Y. Sako (RIKEN, Japan). Cells were maintained in DMEM supplemented with 10% horse serum and 5% fetal bovine serum. A selected clone of HeLa cells, in which chromosome segregation errors are less frequent, was provided by M. Ohsugi (University of Tokyo, Japan) and maintained in DMEM supplemented with 10% fetal bovine serum (Ohsugi et al., 2008). For microscopy experiments, cells were plated on poly-L-lysine-coated coverslips or glass-bottomed dishes, cultured for 12 hours and then serum-starved for at least 16 hours in DMEM without phenol red supplemented with 1% BSA (DMEM-BSA).

Immunofluorescence

Cells were plated on poly-L-lysine-coated coverslips or gridded glass-bottomed dishes, serum starved and stimulated with the indicated concentrations of EGF. Cells were fixed with 4% paraformaldehyde for 10 min at RT, permeabilized in 0.2% Triton X-100 for 10 min at RT or 100% methanol for 10 min at –20°C and then blocked with 1% BSA for 30 min at RT. Cells were then incubated cells primary antibodies (anti-Nup153 (7A8, dilution 1:10), anti-ERK1 (Y72, 1:200), anti-ERK2 (D-2, 1:100), anti-phospho-ERK1/2 (E10, 1:200) antibodies) for 1 – 2 h at RT, followed by secondary antibodies (Alexa Fluor 647 anti-mouse IgG (1:500), Alexa Fluor 488 anti-rabbit IgG (1:1,000), Alexa Fluor 555 anti-mouse IgG2b (1:1,000), Alexa Fluor 647

anti-mouse IgG1 (1:1,000) antibodies) for 1 h at RT.

Live cell imaging

Cells were plated on poly-l-lysine-coated glass bottomed dishes and serum starved. Before microscopy experiments the medium was exchanged to DMEM-BSA containing 10 mM PIPES (pH 7.4). Intracellular distributions of GFP-ERK2 and H2B-mRFP1 proteins were observed using a scanning confocal microscope with a 60×/1.49NA oil immersion objective. Cells were stimulated with the indicated concentrations of EGF or NGF on the microscope and time-lapse movies were obtained at a time resolution of 1 min. For the experiments using inhibitors, cells were treated with 10 μM U0126 or 60 μM FR180204 for 30 min before growth factor stimulation.

Purification of recombinant proteins

The plasmid pGEX-GFP-ERK2-His was transformed into *E. coli* Rosetta, grown in LB medium and expression was induced for 12 hours at 20°C by the addition of 0.1 mM IPTG. For preparation of GFP-ppERK2-His, *E. coli* BL21(DE3) was co-transformed with pGEX-GFP-ERK2-His and pACYC184-Venus-MEK1 (S218/222E, Δ32-51), grown in 2×YT medium and expression was induced for 12 hours at 20°C by the addition of 0.1 mM IPTG. Before harvesting, cells were shaken for 1 – 3 hours at 37°C to enhance ERK2 phosphorylation. Phosphorylation of GFP-ERK2 was confirmed by Phos-tag Western blotting. Protein extracts were incubated with Glutathione Sepharose 4B and GST-tag fused to recombinant proteins was

cleaved by PreScission protease. Recombinant proteins were further purified with cOmplete His-tag Purification Resin (Roche) to concentrate full-length GFP-ERK2 protein. Purified proteins were dialyzed against 20 mM HEPES (pH 7.3), 110 mM KOAc, 1 mM EGTA and 2 mM DTT.

In vitro import assay

Cells were plated on μ-slides (ibidi) and serum starved. Preparation of digitonin-permeabilized cells were performed essentially as described previously (Kosako et al., 2009). Briefly, cells were incubate cells with 50 μg ml^{-1} digitonin in transport buffer (20 mM HEPES-KOH (pH 7.3), 110 mM KOAc, 2 mM MgOAc, 5 mM NaOAc, 0.5 mM EGTA, 2 mM DTT, 1× PhosSTOP phosphatase inhibitor cocktail, and 1× complete mini EDTA-free protease inhibitors) for 5 min at 4°C. For *in vitro* phosphorylation of nucleoporins by ERK, digitonin-permeabilized cells were incubated with transport buffer containing 1 mM ATP, 15 mM $MgCl_2$, and 500 nM GFP or 500 nM GFP-ppERK2 with or without 60 μM FR180204 for 20 min at RT. After washing the cells with transport buffer, I added transport buffer containing 1 mM ATP, 15 mM $MgCl_2$ and 500 nM GFP-ppERK2 on the microscope, and time-lapse movies were obtained at a time resolution of 5 s.

RNA interference

Stealth Select RNAi oligonucleotide against rat Nup153 (rat Nup153 siRNA-#1 (sense), 5'-ACUUCAGUUUCUGGUCGCAAGAUAA-3') and Stealth RNAi negative control duplex-#2

with medium GC content were purchased from Invitrogen. Cells were transfected with 30 nM siRNA using Lipofectamine 3000 reagent (Invitrogen) according to the manufacturer's protocol and observed 64 h after transfection. The fraction of Nup153-depleted cells was approximately 50% – 90%. Therefore, the cells were fixed immediately after the live cell imaging experiments followed by immunofluorescence using anti-Nup153 antibody to identify cells in which Nup153 was depleted.

Data analysis

To analyze the nuclear translocation of GFP-ERK2, nuclei were detected from H2B-mRFP1 images and nuclear intensities of GFP-ERK2 were measured at each time point using custom-made plug-ins of Fiji/ImageJ (fiji.sc/Fiji). For live cell imaging data analysis, nuclear intensities of GFP-ERK2 were normalized by the mean values before stimulation to obtain fold change increase in stimulus-induced ERK nuclear translocation. For *in vitro* import assay, nuclear intensities were normalized by the intensity of the bulk solution.

Numerical computation of mutual information

The mutual information is defined as $I(R;S) = H(R) - H(R|S) = H(S) - H(S|R)$, where $H(X) = \sum_i p(x_i) \log_2 p(x_i)$ represents the entropy. Direct computation of the mutual information is often biased because of the finite (limited) data. Therefore, unbiased value of the mutual information was estimated using an approximated linear relation defined as $I_{\text{biased}} \approx$

$I_\infty + \frac{a_1}{N}$, where N is the total number of samples, a_1 is a coefficient that depends on R and S, and I_{biased} and I_∞ are the biased and unbiased estimate of the mutual information, respectively (Cheong et al., 2011). The linear function was estimated by changing N from 60% – 100% of the total number of data using jackknife sampling, to obtain the unbiased estimate of the mutual information (Cheong et al., 2011).

Kinetic modeling of ERK nuclear translocation

Equations and parameters are listed in Tables 2 – 4. Ordinary differential equations were numerically computed using the routines implemented in the scipy.integrate package (http://docs.scipy.org/doc/scipy/reference/integrate.html). Parameter fitting to the experimental data was carried out based on optimization routines implemented in the scipy.optimize package (http://docs.scipy.org/doc/scipy/reference/optimize.html). Sensitivity coefficient s_i is defined as $s_i = \frac{\partial \ln q}{\partial \ln p_i}$, where q is a target function and p_i is the *i*th parameter (Nakakuki et al., 2010). In this study, the target function was the Hill coefficient of the dose–response relation of ERK nuclear translocation. The sensitivity coefficients were calculated by making 1% changes in each model parameter.

Table 2: Rate equations of the model.

Reaction	Description
$v1 = k_1\, S$	Input signal
$v2 = k_2\, S^*$	Decay of signal
$v3 = k_3\, S^* \dfrac{ERK_{cyt}}{k_3' + ERK_{cyt}}$	ERK phosphorylation
$v4 = k_4\, ppERK_{cyt}$	ERK dephosphorylation in the cytoplasm
$v5 = k_5 \dfrac{ppERK_{cyt}}{k_5' + ppERK_{cyt}}$	Negative feedback to signal (Sos)
$v6 = k_6\, ERK_{cyt}$	ERK nuclear import
$v7 = k_7\, ERK_{nuc}$	ERK nuclear export
$v8 = k_8 \dfrac{ppERK_{cyt}}{k_8' + ppERK_{cyt}} (1 + K\, pNup)$	ppERK nuclear import
$v9 = k_9 \dfrac{ppERK_{nuc}}{k_9' + ppERK_{nuc}} (1 + K\, pNup)$	ppERK nuclear export
$v10 = k_{10}\, ppERK_{nuc}$	ERK dephosphorylation in the nucleus
$v11 = k_{11}\, (v8 + v9) \dfrac{Nup}{k_{11}' + Nup}$	Nup phosphorylation
$v12 = k_{12}\, pNup$	Nup dephosphorylation
$v13 = k_{13}\, ppERK_{nuc}\, Sub$	Association of ppERK and substrate
$v14 = k_{14}\, ppERK\_Sub$	Dissociation of ppERK–substrate complex
$v15 = k_{15}\, ppERK\_Sub$	Substrate phosphorylation
$v16 = k_{16}\, pSub$	Substrate dephosphorylation

Table 3: Equations and initial conditions.

Species	$d/dt =$	Initial value[1]
S	$-v1$	$S_0 = EGF/(k_0' + EGF)$
S^*	$v1 - v2 - v5$	0
ERK_{cyt}	$-v3 + v4 - v6 + v7$	480,000[2]
ERK_{nuc}	$v6 - v7 - v10$	96,000[2]
$ppERK_{cyt}$	$v3 - v4 - v8 + v9$	0
$ppERK_{nuc}$	$v8 - v9 - v10 - v14 + v15 + v16$	0
Nup	$-v11 + v12$	5,000[3]
$pNup$	$v11 - v12$	0
Sub	$-v13 + v14 + v16$	96,000[4]
$ppERK\_Sub$	$v13 - v14 - v15$	0
$pSub$	$v15 - v16$	0

[1] Assuming that the cell volume was 1 pl (Fujioka et al., 2006). [2] Total number of ERK molecules was assumed to be 576,000 (~0.96 μM (Fujioka et al., 2006)). [3] Assumed based on the literature (Allen et al., 2000; Maeshima et al., 2010). [4] Assumption (relatively determined by parameter fitting).

Table 4: Parameter values.

Parameter	Value[1]
k_0'	0.198 [ng ml^{-1}]
k_1	9.21e-2
k_2	5.90e-2
k_3	8.23e5 [c min^{-1}]
k_3'	9.30e2
k_4	1.01
k_5	2.03e-2
k_5'	3.18e4
k_6	0.18[2]
k_7	0.9[2]
k_8	6.23e4
k_8'	3.47e6
k_9	4.30e4
k_9'	1.41e4
K	2.43e-02 [dimensionless]
k_{10}	3.55e1
k_{11}	1.95 [dimensionless]
k_{11}'	2.46e3
k_{12}	1.60e1
k_{13}	1.12e-3
k_{14}	0.120
k_{15}	0.184
k_{16}	2.86e-6

[1] All units are shown in terms of number of molecules and minute except where otherwise explicitly indicated. c: arbitrary unit of concentration. [2] Assumed based on the literature (Aoki et al., 2011; Reiterer et al., 2013).

References

Ahmed, S., Grant, K.G., Edwards, L.E., Rahman, A., Cirit, M., Goshe, M.B., and Haugh, J.M. (2014). Data-driven modeling reconciles kinetics of ERK phosphorylation, localization, and activity states. Mol. Syst. Biol. *10*, 1–14.

Allen, T.D., Cronshaw, J.M., Bagley, S., Kiseleva, E., and Goldberg, M.W. (2000). The nuclear pore complex: mediator of translocation between nucleus and cytoplasm. J. Cell Sci. *113*, 1651–1659.

Alon, U. (2007). Network motifs: theory and experimental approaches. Nat. Rev. Genet. *8*, 450–461.

Aoki, K., Yamada, M., Kunida, K., Yasuda, S., and Matsuda, M. (2011). Processive phosphorylation of ERK MAP kinase in mammalian cells. Proc. Natl. Acad. Sci. U. S. A. *108*, 12675–12680.

Aoki, K., Kumagai, Y., Sakurai, A., Komatsu, N., Fujita, Y., Shionyu, C., and Matsuda, M. (2013). Stochastic ERK Activation Induced by Noise and Cell-to-Cell Propagation Regulates Cell Density-Dependent Proliferation. Mol. Cell *52*, 529–540.

Brunet, A., Roux, D., Lenormand, P., Dowd, S., Keyse, S., and Pouysségur, J. (1999). Nuclear translocation of p42/p44 mitogen-activated protein kinase is required for growth factor-induced gene expression and cell cycle entry. EMBO J. *18*, 664–674.

Carlson, S.M., Chouinard, C.R., Labadorf, A., Lam, C.J., Schmelzle, K., Fraenkel, E., and White, F.M. (2011). Large-scale discovery of ERK2 substrates identifies ERK-mediated transcriptional regulation by ETV3. Sci. Signal. *4*, rs11.

Caunt, C.J., and McArdle, C.A. (2010). Stimulus-induced uncoupling of extracellular signal-regulated kinase phosphorylation from nuclear localization is dependent on docking domain interactions. J. Cell Sci. *123*, 4310–4320.

Caunt, C.J., and McArdle, C.A. (2012). ERK phosphorylation and nuclear accumulation: insights from single-cell imaging. Biochem. Soc. Trans. *40*, 224–229.

Chang, L., and Karin, M. (2001). Mammalian MAP kinase signalling cascades. Nature *410*, 37–40.

Cheong, R., Rhee, A., Wang, C.J., Nemenman, I., and Levchenko, A. (2011). Information

transduction capacity of noisy biochemical signaling networks. Science *334*, 354–358.

Chuderland, D., Konson, A., and Seger, R. (2008). Identification and characterization of a general nuclear translocation signal in signaling proteins. Mol. Cell *31*, 850–861.

Cohen-Saidon, C., Cohen, A.A., Sigal, A., Liron, Y., and Alon, U. (2009). Dynamics and variability of ERK2 response to EGF in individual living cells. Mol. Cell *36*, 885–893.

Costa, M., Marchi, M., Cardarelli, F., Roy, A., Beltram, F., Maffei, L., and Ratto, G.M. (2006). Dynamic regulation of ERK2 nuclear translocation and mobility in living cells. J. Cell Sci. *119*, 4952–4963.

Czubryt, M.P., Austria, J.A., and Pierce, G.N. (2000). Hydrogen peroxide inhibition of nuclear protein import is mediated by the mitogen-activated protein kinase, ERK2. J. Cell Biol. *148*, 7–16.

Ferrell, J.E., and Ha, S.H. (2014a). Ultrasensitivity part I: Michaelian responses and zero-order ultrasensitivity. Trends Biochem. Sci. *39*, 496–503.

Ferrell, J.E., and Ha, S.H. (2014b). Ultrasensitivity part II: multisite phosphorylation, stoichiometric inhibitors, and positive feedback. Trends Biochem. Sci. *39*, 556–569.

Ferrell, J.E., and Machleder, E.M. (1998). The biochemical basis of an all-or-none cell fate switch in Xenopus oocytes. Science *280*, 895–898.

Formstecher, E., Ramos, J.W., Fauquet, M., Calderwood, D.A., Hsieh, J.C., Canton, B., Nguyen, X.T., Barnier, J.V., Camonis, J., Ginsberg, M.H., et al. (2001). PEA-15 Mediates Cytoplasmic Sequestration of ERK MAP Kinase. Dev. Cell *1*, 239–250.

Frey, S., and Görlich, D. (2007). A Saturated FG-Repeat Hydrogel Can Reproduce the Permeability Properties of Nuclear Pore Complexes. Cell *130*, 512–523.

Fujioka, A., Terai, K., Itoh, R.E., Aoki, K., Nakamura, T., Kuroda, S., Nishida, E., and Matsuda, M. (2006). Dynamics of the Ras/ERK MAPK cascade as monitored by fluorescent probes. J. Biol. Chem. *281*, 8917–8926.

Fukuda, M., Gotoh, Y., and Nishida, E. (1997). Interaction of MAP kinase with MAP kinase kinase: its possible role in the control of nucleocytoplasmic transport of MAP kinase. EMBO J. *16*, 1901–1908.

Götz, M., and Huttner, W.B. (2005). The cell biology of neurogenesis. Nat. Rev. Mol. Cell Biol. *6*,

777–788.

Horgan, A.M., and Stork, P.J.. (2003). Examining the mechanism of Erk nuclear translocation using green fluorescent protein. Exp. Cell Res. *285*, 208–220.

Huang, C.Y., and Ferrell, J.E. (1996). Ultrasensitivity in the mitogen-activated protein kinase cascade. Proc. Natl. Acad. Sci. U. S. A. *93*, 10078–10083.

Kamioka, Y., Yasuda, S., Fujita, Y., Aoki, K., and Matsuda, M. (2010). Multiple decisive phosphorylation sites for the negative feedback regulation of SOS1 via ERK. J. Biol. Chem. *285*, 33540–33548.

Kanda, T., Sullivan, K.F., and Wahl, G.M. (1998). Histone-GFP fusion protein enables sensitive analysis of chromosome dynamics in living mammalian cells. Curr. Biol. *8*, 377–385.

Kholodenko, B.N. (2000). Negative feedback and ultrasensitivity can bring about oscillations in the mitogen-activated protein kinase cascades. Eur. J. Biochem. *267*, 1583–1588.

Kim, E.K., and Choi, E.-J. (2010). Pathological roles of MAPK signaling pathways in human diseases. Biochim. Biophys. Acta *1802*, 396–405.

Kimura, H., and Cook, P.R. (2001). Kinetics of core histones in living human cells: little exchange of H3 and H4 and some rapid exchange of H2B. J. Cell Biol. *153*, 1341–1353.

Kosako, H., Yamaguchi, N., Aranami, C., Ushiyama, M., Kose, S., Imamoto, N., Taniguchi, H., Nishida, E., and Hattori, S. (2009). Phosphoproteomics reveals new ERK MAP kinase targets and links ERK to nucleoporin-mediated nuclear transport. Nat. Struct. Mol. Biol. *16*, 1026–1035.

Lee, T., Hoofnagle, A.N., Kabuyama, Y., Stroud, J., Min, X., Goldsmith, E.J., Chen, L., Resing, K.A., and Ahn, N.G. (2004). Docking motif interactions in MAP kinases revealed by hydrogen exchange mass spectrometry. Mol. Cell *14*, 43–55.

Lidke, D.S., Huang, F., Post, J.N., Rieger, B., Wilsbacher, J., Thomas, J.L., Pouysségur, J., Jovin, T.M., and Lenormand, P. (2010). ERK nuclear translocation is dimerization-independent but controlled by the rate of phosphorylation. J. Biol. Chem. *285*, 3092–3102.

Lorenzen, J.A., Baker, S.E., Denhez, F., Melnick, M.B., Brower, D.L., and Perkins, L.A. (2001). Nuclear import of activated D-ERK by DIM-7, an importin family member encoded by the gene moleskin. Development *128*, 1403–1414.

Luckheeram, R.V., Zhou, R., Verma, A.D., and Xia, B. (2012). CD4+T Cells: Differentiation and Functions. Clin. Dev. Immunol. *2012*, 1–12.

MacKeigan, J.P., Murphy, L.O., Dimitri, C.A., and Blenis, J. (2005). Graded mitogen-activated protein kinase activity precedes switch-like c-Fos induction in mammalian cells. Mol. Cell. Biol. *25*, 4676–4682.

Maeshima, K., Iino, H., Hihara, S., Funakoshi, T., Watanabe, A., Nishimura, M., Nakatomi, R., Yahata, K., Imamoto, F., Hashikawa, T., et al. (2010). Nuclear pore formation but not nuclear growth is governed by cyclin-dependent kinases (Cdks) during interphase. Nat. Struct. Mol. Biol. *17*, 1065–1071.

Markevich, N.I., Hoek, J.B., and Kholodenko, B.N. (2004). Signaling switches and bistability arising from multisite phosphorylation in protein kinase cascades. J. Cell Biol. *164*, 353–359.

Matsubayashi, Y., Fukuda, M., and Nishida, E. (2001). Evidence for existence of a nuclear pore complex-mediated, cytosol-independent pathway of nuclear translocation of ERK MAP kinase in permeabilized cells. J. Biol. Chem. *276*, 41755–41760.

Michailovici, I., Harrington, H.A., Azogui, H.H., Yahalom-Ronen, Y., Plotnikov, A., Ching, S., Stumpf, M.P.H., Klein, O.D., Seger, R., and Tzahor, E. (2014). Nuclear to cytoplasmic shuttling of ERK promotes differentiation of muscle stem/progenitor cells. Development *141*, 2611–2620.

Nakakuki, T., Birtwistle, M.R., Saeki, Y., Yumoto, N., Ide, K., Nagashima, T., Brusch, L., Ogunnaike, B.A., Okada-Hatakeyama, M., and Kholodenko, B.N. (2010). Ligand-specific c-Fos expression emerges from the spatiotemporal control of ErbB network dynamics. Cell *141*, 884–896.

Ohori, M., Kinoshita, T., Okubo, M., Sato, K., Yamazaki, A., Arakawa, H., Nishimura, S., Inamura, N., Nakajima, H., Neya, M., et al. (2005). Identification of a selective ERK inhibitor and structural determination of the inhibitor-ERK2 complex. Biochem. Biophys. Res. Commun. *336*, 357–363.

Ohsugi, M., Adachi, K., Horai, R., Kakuta, S., Sudo, K., Kotaki, H., Tokai-Nishizumi, N., Sagara, H., Iwakura, Y., and Yamamoto, T. (2008). Kid-Mediated Chromosome Compaction Ensures Proper Nuclear Envelope Formation. Cell *132*, 771–782.

Patel, S.S., Belmont, B.J., Sante, J.M., and Rexach, M.F. (2007). Natively Unfolded Nucleoporins Gate Protein Diffusion across the Nuclear Pore Complex. Cell *129*, 83–96.

Pellettieri, J., and Alvarado, A.S. (2007). Cell Turnover and Adult Tissue Homeostasis: From Humans to Planarians. Annu. Rev. Genet. *41*, 83–105.

Perrett, R.M., Fowkes, R.C., Caunt, C.J., Tsaneva-Atanasova, K., Bowsher, C.G., and McArdle, C.A. (2013). Signaling to extracellular signal-regulated kinase from ErbB1 kinase and protein kinase C: feedback, heterogeneity, and gating. J. Biol. Chem. *288*, 21001–21014.

Plotnikov, A., Chuderland, D., Karamansha, Y., Livnah, O., and Seger, R. (2011). Nuclear extracellular signal-regulated kinase 1 and 2 translocation is mediated by casein kinase 2 and accelerated by autophosphorylation. Mol. Cell. Biol. *31*, 3515–3530.

Plotnikov, A., Flores, K., Maik-rachline, G., Zehorai, E., Kapri-pardes, E., Berti, D.A., Hanoch, T., Besser, M.J., and Seger, R. (2015). The nuclear translocation of ERK1/2 as an anticancer target. Nat. Commun. *6*, 6685.

Pomerening, J.R., Sontag, E.D., and Ferrell, J.E. (2003). Building a cell cycle oscillator: hysteresis and bistability in the activation of Cdc2. Nat. Cell Biol. *5*, 346–351.

Qi, M., and Elion, E.A. (2005). MAP kinase pathways. J. Cell Sci. *118*, 3569–3572.

Qian, H. (2012). Cooperativity in Cellular Biochemical Processes: Noise-Enhanced Sensitivity, Fluctuating Enzyme, Bistability with Nonlinear Feedback, and Other Mechanisms for Sigmoidal Responses. Annu. Rev. Biophys. *41*, 179–204.

Qiao, L., Nachbar, R.B., Kevrekidis, I.G., and Shvartsman, S.Y. (2007). Bistability and oscillations in the Huang-Ferrell model of MAPK signaling. PLoS Comput. Biol. *3*, 1819–1826.

Reiterer, V., Fey, D., Kolch, W., Kholodenko, B.N., and Farhan, H. (2013). Pseudophosphatase STYX modulates cell-fate decisions and cell migration by spatiotemporal regulation of ERK1/2. Proc. Natl. Acad. Sci. U. S. A. *110*, E2934–E2943.

Roux, P.P., and Blenis, J. (2004). ERK and p38 MAPK-Activated Protein Kinases : a Family of Protein Kinases with Diverse Biological Functions. Microbiol. Mol. Biol. Rev. *68*, 320–344.

Santos, S.D.M., Verveer, P.J., and Bastiaens, P.I.H. (2007). Growth factor-induced MAPK network topology shapes Erk response determining PC-12 cell fate. Nat. Cell Biol. *9*, 324–330.

Shinohara, H., Behar, M., Inoue, K., Hiroshima, M., Yasuda, T., Nagashima, T., Kimura, S., Sanjo, H., Maeda, S., Yumoto, N., et al. (2014). Positive feedback within a kinase signaling complex functions as a switch mechanism for NF-κB activation. Science *344*, 760–764.

Skotheim, J.M., Di Talia, S., Siggia, E.D., and Cross, F.R. (2008). Positive feedback of G1 cyclins ensures coherent cell cycle entry. Nature *454*, 291–296.

Takahashi, M., Shibata, T., Yanagida, T., and Sako, Y. (2012). A protein switch with tunable steepness reconstructed in Escherichia coli cells with eukaryotic signaling proteins. Biochem. Biophys. Res. Commun. *421*, 731–735.

Torii, S., Kusakabe, M., Yamamoto, T., Maekawa, M., and Nishida, E. (2004). Sef Is a Spatial Regulator for Ras/MAP Kinase Signaling. Dev. Cell *7*, 33–44.

Tyson, J.J., Chen, K.C., and Novak, B. (2003). Sniffers, buzzers, toggles and blinkers: Dynamics of regulatory and signaling pathways in the cell. Curr. Opin. Cell Biol. *15*, 221–231.

Vaudry, D., Stork, P.J.S., Lazarovici, P., and Eiden, L.E. (2002). Signaling pathways for PC12 cell differentiation: making the right connections. Science *296*, 1648–1649.

Velnar, T., Bailey, T., and Smrkolj, V. (2009). The wound healing process: an overview of the cellular and molecular mechanisms. J. Int. Med. Res. *37*, 1528–1542.

Vomastek, T., Iwanicki, M.P., Burack, W.R., Tiwari, D., Kumar, D., Parsons, J.T., Weber, M.J., and Nandicoori, V.K. (2008). Extracellular signal-regulated kinase 2 (ERK2) phosphorylation sites and docking domain on the nuclear pore complex protein Tpr cooperatively regulate ERK2-Tpr interaction. Mol. Cell. Biol. *28*, 6954–6966.

Wente, S.R., and Rout, M.P. (2010). The Nuclear Pore Complex and Nuclear Transport. Cold Spring Harb. Perspect. Biol. *2*, a000562.

Whitehurst, A., Cobb, M.H., and White, M.A. (2004). Stimulus-Coupled Spatial Restriction of Extracellular Signal-Regulated Kinase 1/2 Activity Contributes to the Specificity of Signal-Response. Mol. Cell. Biol. *24*, 10145–10150.

Whitehurst, A.W., Wilsbacher, J.L., You, Y., Luby-phelps, K., Moore, M.S., and Cobb, M.H. (2002). ERK2 enters the nucleus by a carrier- independent mechanism. Proc. Natl. Acad. Sci. U. S. A. *99*, 7496–7501.

Widmann, C., Gibson, S., Jarpe, M.B., and Johnson, G.L. (1999). Mitogen-activated protein kinase: conservation of a three-kinase module from yeast to human. Physiol. Rev. *79*, 143–180.

Wood, W., Turmaine, M., Weber, R., Camp, V., Maki, R.A., McKercher, S.R., and Martin, P. (2000). Mesenchymal cells engulf and clear apoptotic footplate cells in macrophageless PU.1 null

mouse embryos. Development *127*, 5245–5252.

Xiong, W., and Ferrell, J.E. (2003). A positive-feedback-based bistable “memory module” that governs a cell fate decision. Nature *426*, 460–465.

Yoon, S., and Seger, R. (2006). The extracellular signal-regulated kinase: multiple substrates regulate diverse cellular functions. Growth Factors *24*, 21–44.

Zhang, Q., Bhattacharya, S., and Andersen, M.E. (2013). Ultrasensitive response motifs: basic amplifiers in molecular signalling networks. Open Biol. *3*, 130031.

Achievements

Papers

1. Shindo Y, Iwamoto K, Mouri K, Hibino K, Tomita M, Kosako H, Sako Y, Takahashi K. Conversion of graded phosphorylation into switch-like nuclear translocation via autoregulatory mechanisms in ERK signalling. *Nature Communications* **7**, 10485 (2016).

2. Watabe M, Arjunan SNV, Fukushima S, Iwamoto K, Kozuka J, Matsuoka S, Shindo Y, Ueda M, Takahashi K. A computational framework for bioimaging simulation. *PLOS ONE* **10**, e0130089 (2015).

3. Shindo Y, Nozaki T, Saito R, Tomita M. Computational analysis of associations between alternative splicing and histone modifications. *FEBS Letters* **587**, 516–521 (2013).

Selected conference presentations

1. 新土優樹，岩本一成，毛利一成，日比野佳代，冨田勝，小迫英尊，佐甲靖志，高橋恒一. EGF 刺激に対する ERK の核移行応答は自己制御を伴いスイッチ様に振る舞う. BMB2015（第 38 回日本分子生物学会年会，第 88 回日本生化学会大会合同年会），神戸，2015 年 12 月.

2. Shindo Y, Mouri K, Hibino K, Iwamoto K, Sako Y, Takahashi K. Switch-like behavior of EGF-induced ERK nuclear translocation in mammalian cells as observed by live cell fluorescence imaging. *International Conference on Systems Biology 2014*, Melbourne, Australia, September 2014.

3. Iwamoto K, Shindo Y, Takahashi K. Cellular noise generating heterogeneity in epidermal growth factor signalling pathway. *International Conference on Systems Biology 2015* Biopolis, Singapore, September 2015.

4. Iwamoto K, Shindo Y, Miyauchi A, Takahashi K. Particle simulation of EGF signalling pathway under cellular environment. *International Conference on Systems Biology 2014*, Melbourne, Australia, September 2014.

Awards

1. 若手優秀発表賞，BMB2015（第38回日本分子生物学会年会，第88回日本生化学会大会合同年会）

Fellowships

1. 日本学術振興会　特別研究員DC1（2014年4月 – ）